splicing initiation U2 snRNP is brought to the 3' splice site. This

involves base pairing of the U2 RNA to the branch site RNA (9)

and localization of the SF3b subunit p14 near the branch point

adenosine by an interaction with the N terminus of the U2

snRNP component SF3b155 (10-12). Initial contacts between

the U2 snRNP and the pre-mRNA are mediated by the N ter-

minus of SF3b155 binding to U2AF<sup>65</sup> and displacing SF1 from

RRM of U2AF35 share distinct sequence features that are not

found in canonical RRMs and mediate binding to tryptophan-

containing peptide sequences in cognate splicing factors (14-

19). These noncanonical RRMs form a subgroup of RRMs

The third RNA recognition motif (RRM)<sup>3</sup> of U2AF<sup>65</sup> and the

the branch point sequence (13).

## Dimerization and Protein Binding Specificity of the U2AF Homology Motif of the Splicing Factor Puf60\*5

Received for publication, July 16, 2008, and in revised form, October 7, 2008 Published, JBC Papers in Press, October 29, 2008, DOI 10.1074/jbc.M805395200

Lorenzo Corsini<sup>‡</sup>, Michael Hothorn<sup>‡1</sup>, Gunter Stier<sup>‡</sup>, Vladimir Rybin<sup>‡</sup>, Klaus Scheffzek<sup>‡</sup>, Toby J. Gibson<sup>‡</sup>, and Michael Sattler \*§ ¶2

From the <sup>‡</sup>Structural and Computational Biology Unit, European Molecular Biology Laboratory, Meyerhofstrasse 1, 69117 Heidelberg, Germany, the  $^\S$ Institute of Structural Biology, Helmholtz Zentrum München, Ingolstädter Landstrasse 1, 85764 Neuherberg, Germany, and the ¶Munich Center for Integrated Protein Science and Chair Biomolecular NMR, Department Chemie, Technische Universität München, Lichtenbergstrasse 4, 85747 Garching, Germany

PUF60 is an essential splicing factor functionally related and homologous to U2AF<sup>65</sup>. Its C-terminal domain belongs to the family of U2AF (U2 auxiliary factor) homology motifs (UHM), a subgroup of RNA recognition motifs that bind to tryptophancontaining linear peptide motifs (UHM ligand motifs, ULMs) in several nuclear proteins. Here, we show that the Puf60 UHM is mainly monomeric in physiological buffer, whereas its dimerization is induced upon the addition of SDS. The crystal structure of PUF60-UHM at 2.2 Å resolution, NMR data, and mutational analysis reveal that the dimer interface is mediated by electrostatic interactions involving a flexible loop. Using glutathione S-transferase pulldown experiments, isothermal titration calorimetry, and NMR titrations, we find that Puf60-UHM binds to ULM sequences in the splicing factors SF1, U2AF<sup>65</sup>, and SF3b155. Compared with U2AF<sup>65</sup>-UHM, Puf60-UHM has distinct binding preferences to ULMs in the N terminus of SF3b155. Our data suggest that the functional cooperativity between U2AF<sup>65</sup> and Puf60 may involve simultaneous interactions of the two proteins with SF3b155.

Pre-mRNA splicing is a stepwise process initiated by the recognition of sequence elements at the splice site by specific splicing factors (1). The branch point sequence is recognized by splicing factor SF1 (2, 3), whereas the polypyrimidine tract and the 3' splice site AG-dinucleotide are bound by the heterodimer U2AF<sup>65</sup>-U2AF<sup>35</sup> (4-7). Although SF1 alone interacts only weakly with the branch point sequence, this interaction is stabilized significantly by U2AF<sup>65</sup>, which binds simultaneously to SF1 and to the polypyrimidine tract (8). In the next step of

SF3b155 (13, 23).

PUF60 (poly-<u>U</u>-binding <u>factor</u> <u>60</u> kDa, also called FIR, Hfp, Ro-bp1) is a splicing factor homologous to and complementary in function to U2AF<sup>65</sup>. Similarly to U2AF<sup>65</sup>, its domain structure consists of a predicted intrinsically unstructured N terminus, two central RRM domains, and a C-terminal UHM. The UHM domain is special in that it has been reported to mediate homodimerization of Puf60 in SDS-PAGE (21). Full-length Puf60 was found to interact with itself in yeast two-hybrid analyses, suggesting that the oligomerization detected in SDS-PAGE also occurs under physiological conditions (26, 27).

ously identify a functional ULM. Candidate ULMs are found

in many proteins, but a biological function has so far been assigned only to those in U2AF<sup>65</sup> (17, 25), SF1 (16, 23), and

<sup>&</sup>lt;sup>3</sup> The abbreviations used are: RRM, RNA recognition motif; UHM, U2AF homology motif; ULM, UHM ligand motif; GST, glutathione S-transferase; HSQC, heteronuclear single quantum coherence; NOE, nuclear Overhauser effect; AUC, analytical ultracentrifugation; Trx, thioredoxin A; ITC, isothermal titration calorimetry.



called U2AF homology motif (UHM) (20). UHMs in other splicing factors have also been shown to bind to short tryptophan-containing linear motifs in U2AF<sup>65</sup>, SF1, and SF3b155 (21-24), which are thus called UHM ligand motifs (ULM) (23). High resolution structures of protein peptide complexes involving U2AF<sup>35</sup>-UHM/U2AF<sup>65</sup>-ULM (14), U2AF<sup>65</sup>-UHM/ SF1-ULM (15), and the UHM of SPF45 (splicing factor 45 kDa) bound to an ULM in SF3b155 (23) all share a very similar mode of molecular recognition, suggesting that UHMs in other proteins might bind similar linear motifs as well. Because the ULM consensus motif is rather short ((K/R) $_{4-6}X_{0-1}$ W(D/E/N/Q) $_{1-2}$ ), its mere presence in a protein sequence cannot unambigu-

<sup>\*</sup> This work was supported by Deutsche Forschungsgemeinschaft Grant Sa 823/5 and European Commission 3D Repertoire Grant LSHG-CT-2005-512028, and funds from the Peter and Traudl Engelhorn Foundation (to M. H.). The costs of publication of this article were defraved in part by the payment of page charges. This article must therefore be hereby marked "advertisement" in accordance with 18 U.S.C. Section 1734 solely to indicate this fact.

The on-line version of this article (available at http://www.jbc.org) contains supplemental Fig. S1-S5.

The atomic coordinates and structure factors (code 3DXB) have been deposited in the Protein Data Bank, Research Collaboratory for Structural Bioinformatics, Rutgers University, New Brunswick, NJ (http://www.rcsb.org/).

<sup>&</sup>lt;sup>1</sup> Present address: Plant Biology Laboratory, The Salk Institute, La Jolla, CA

<sup>&</sup>lt;sup>2</sup> To whom correspondence should be addressed. Tel.: 49-89-289-13418; Fax: 49-89-289-13869; E-mail: sattler@helmholtz-muenchen.de.

Puf60 was discovered as a poly-U RNA-binding protein required to reconstitute splicing in depleted nuclear extracts. Its function is enhanced by the presence of U2AF<sup>65</sup>, but not by the small U2AF subunit, U2AF35 (21). Puf60 and U2AF65 can interact in vitro and in yeast cells (21, 26, 27). It was recently demonstrated that Puf60 and U2AF65 mutually enhance their affinity for binding polypyrimidine tract RNA in a cooperative fashion. Moreover, the ratio of U2AF<sup>65</sup> to Puf60 can directly influence selective inclusion or skipping of alternatively spliced exons in several genes (28). The function of Puf60 in splicing is thus closely linked to the function of U2AF<sup>65</sup>.

In addition to its role in alternative splicing, Puf60 also controls human c-myc gene expression. Under the synonym FIR (FBP-interacting repressor), Puf60 was reported to interact with and inhibit the transcription factor FBP (FUSE (far upstream sequence element)-binding-protein), an activator of c-myc promoters (29). Probably because of a similar mechanism, mutations in the *Drosophila* homolog of Puf60, Hfp (Half Pint), lead to increased expression of d-myc genes, thus negatively regulating cell cycle progression (30). Hfp mutations also lead to aberrant splicing of specific mRNAs in *Drosophila* ovaries (31). Similar to its mammalian ortholog Puf60, Hfp is thus a regulator both of transcription and of alternative splicing.

Here, we report that Puf60 UHM is mainly monomeric under physiological conditions, whereas it dimerizes upon the addition of SDS. The crystal structure of PUF60-UHM and mutational analysis reveal that the dimerization is entirely mediated by electrostatic interactions. NMR relaxation data show that the dimer interface involves a loop that is highly flexible in solution. Furthermore, we show that PUF60-UHM binds to ULM sequences in U2AF<sup>65</sup>, SF1, and SF3b155. The UHMs in PUF60 and U2AF<sup>65</sup> show preferences for binding to different ULMs in the N terminus of SF3b155. We propose that PUF60 and U2AF65 may cooperatively recruit U2 snRNP by simultaneously binding to SF3b155.

#### **EXPERIMENTAL PROCEDURES**

Protein Preparation-Recombinant Puf60-UHM (residues 460 – 559, wild type, and mutants), thioredoxin-Puf60-UHM, SPF45-UHM(301-401), U2AF<sup>35</sup>-UHM (residues 38-152), and U2AF<sup>65</sup>-UHM (residues 369-475) were expressed from modified pET9d vectors with a noncleavable N-terminal His, tag.  $U2AF^{65}(85-112)$ , SF1(1-25), SF3b155(1-424, 194-229, 210-124)251, 229 – 269, 284 – 307, 317 – 357, wild type, and mutants), and Prp16 (1-314, 201-238, wild type, and mutants) were expressed from modified pET9d vectors with tobacco etch virus protease cleavable, N-terminal His6, and glutathione S-transferase (GST) tags. Unlabeled proteins were expressed in Escherichia coli BL21(DE3)pLysS in LB medium. All of the proteins were purified with nickel-nitrilotriacetic acid-agarose (Qiagen) under standard conditions and buffer exchanged to phosphate-buffered saline. For the preparation of ULM peptides for NMR titrations see the supplemental data. Isotopically <sup>13</sup>C- and/or <sup>15</sup>N-labeled proteins were expressed in minimal (M9) medium supplemented with <sup>13</sup>C-D-glucose and/or <sup>15</sup>NH<sub>4</sub>Cl. NMR samples were concentrated to 0.3−1.0 m<sub>M</sub> in 20 mm Na<sub>2</sub>PO<sub>4</sub> buffer (pH 6.8), 150 mm NaCl, and 5 mm β-mercaptoethanol. The samples used for crystallization were additionally purified by size exclusion chromatography on a Superdex<sup>TM</sup> 75 16/60 prep grade column.

NMR—All of the NMR spectra were recorded at 300 K on a Bruker DRX500 spectrometer, processed with NMRPipe (32), and analyzed with NMRView (33). Backbone <sup>1</sup>H, <sup>15</sup>N, and <sup>13</sup>C resonances were assigned with standard triple resonance experiments (34). <sup>15</sup>N relaxation data were recorded as described (35). Dissociation constants were derived from chemical shift displacements in HSQC spectra upon the addition of ligands as described (36) (see supplemental data).

Crystallization and Data Collection—For crystallization, the chimeric thioredoxin-Puf60(460-559) fusion protein was concentrated to about 70 mg/ml in 20 mm Tris (pH 7.0), 150 mm NaCl, 5 mm  $\beta$ -mercaptoethanol. The crystals were grown by vapor diffusion from hanging drops composed of 1  $\mu$ l of protein solution and 1  $\mu$ l of crystallization buffer (1.4 M (NH<sub>4</sub>)<sub>2</sub>SO<sub>4</sub>, 50 mm potassium formate) suspended over 1 ml of the latter as reservoir solution. The crystals grew to sizes of about 100  $\times$  $100 \times 500 \,\mu \text{m}$  and were cryoprotected by serial transfer into a solution containing 20% (v/v) ethylene glycol, 1.5 M (NH<sub>4</sub>)<sub>2</sub>SO<sub>4</sub>, 50 mm potassium formate). Diffraction data were recorded at beam-line PX01 of the Swiss Light Source (Villigen, Switzerland). Data processing and scaling was carried out with XDS (37).

Structure Determination and Refinement—The structure of the thioredoxin-Puf60 fusion protein was solved by molecular replacement as implemented in PHASER (38). The structure of E. coli thioredoxin (Protein Data Bank code 2TRX) and a homology model of Puf60-UHM generated with MODELLER (39) based on the structure of free SPF45-UHM (Protein Data Bank code 2PE8) as a template were used as search models. The solution comprises eight Trx-Puf60-UHM monomers that were refined in alternating cycles of model correction in COOT (40), and restrained refinement as implemented in REFMAC (41) and PHENIX.REFINE (Ref. 42; see Table 1 for structural statistics). Structures were visualized with PYMOL (DeLano Scientific LLC, San Carlos, CA). The eight UHM domains in the unit cell of the crystal structure can be superimposed onto a reported solution structure of Puf60-UHM (Protein Data Bank code 2DNY) with root mean square deviations of 0.9-1.1 Å over 90 of 100 C $\alpha$  atoms. The solution structure, however, does not indicate dimerization of the Puf60-UHM.

GST Pulldown Experiments—GST-tagged ULMs (1 nmol) were mixed with 3 nmol of His<sub>6</sub>-tagged UHMs in 150 μl of phosphate-buffered saline supplemented with 2 mm β-mercaptoethanol and 0.1% (w/v) Igepal CA-630 at 22 °C and mixed vigorously for 1 h. For GST precipitation, 8 μl of glutathione-Sepharose 4B (Amersham Biosciences) pre-equilibrated in phosphate-buffered saline were added and mixed vigorously for 30 min. The beads were washed three times for 1 min in the buffer described above and analyzed by SDS-PAGE. Western blotting was carried out with  $\alpha$ -Puf60 antibody (Abcam 22819).

#### **RESULTS**

Puf60-UHM Is Mainly Monomeric in Physiological Buffer— Puf60 interacts with itself in yeast two-hybrid analyses (26, 27), and its C-terminal UHM domain has been shown to form dimers resistant to denaturing SDS-PAGE (21). We used NMR spectroscopy to characterize the oligomerization state of



TABLE 1 Summary of crystallographic analysis

The values in parentheses indicate the highest resolution shell.

Data collection	
Space group	P2 <sub>1</sub> 2 <sub>1</sub> 2 <sub>1</sub> (19)
Unit cell dimensions	a = 75.12; b = 89.42; c = 299.39;
	$lpha=eta=\gamma=90^\circ$
Wavelength (Å)	1.006
Resolution range (Å)	49.75-2.20 (2.33-2.20)
Unique reflections	102,915 (16265)
Redundancy	6.1 (5.8)
$< I > /\sigma(I)^a$	14.54 (3.21)
$R_{\rm meas}$ (%) $^a$	10.4 (60.6)
Completeness (%)	99.8 (98.9)
Refinement	
Resolution range (Å)	49.75-2.20
$R_{\text{work}}/R_{\text{free}}^{\ \ \ \ \ \ \ \ \ \ \ \ \ \ \ \ \ \ \ $	0.211/0.271
No. of atoms	**********
Protein	13,138
Water	1209
Mean B-factors (Å <sup>2</sup> ) <sup>c</sup>	120)
Thioredoxin domains	22.44
Puf60-UHM domains	20.13
Water	35.21
Root mean square deviations	33.21
Bond lengths (Å)	0.006
Angles (°)	1.012
Ramachandran <sup>d</sup>	11012
Most favored (# (%))	1387 (92.3%)
Additionally allowed (# (%))	106 (7.1%)
Generously allowed (# (%))	2 (0.1%)
Disallowed (# (%))	7 (0.5%)
- ( (,	, · · · · · · · ·

<sup>&</sup>lt;sup>a</sup> As defined in XDS (37).

Puf60-UHM in solution (50 mм P<sub>i</sub>, pH 7.0, 150 mм NaCl, 5 mм dithiothreitol). NMR secondary chemical shifts (Fig. 1A) show that Puf60-UHM adopts the typical  $\beta$ 1- $\alpha$ A- $\beta$ 2- $\beta$ 3- $\alpha$ B- $\beta$ 4- $\alpha$ C topology found for all RRMs and UHMs (20, 43). The overall rotational correlation time  $(\tau_c)$  of Puf60-UHM was calculated from the ratio of the trimmed mean  $^{15}$ N longitudinal ( $T_1$ ) and transverse  $(T_2)$  relaxation times of residues with heteronuclear <sup>1</sup>H-<sup>15</sup>N NOE values above 0.65 (Fig. 1*B*) (44, 45). The average  $^{15}$ N  $T_1/T_2$  ratio for these residues is 7.4 (Fig. 1*C*), corresponding to a  $\tau_c$  of 9.7 ns. However, at 50 MHz Larmor frequency and 297 K,  $\tau_c$  values of 8.3 ns  $(T_1/T_2 = 5.7)$  and 15.8 ns  $(T_1/T_2 =$ 17.7) would be expected for a 13-kDa monomer and a 26-kDa UHM domain dimer, respectively (46, 47) (gray lines in Fig. 1C). Thus, the observed relaxation times indicate the presence of a mainly monomeric rather than a dimeric form of Puf60-UHM. The slightly increased  $T_1/T_2$  ratio, compared with what is expected for a pure monomer, might result from some nonspecific aggregation, because the  $T_1/T_2$  ratio of Puf60-UHM lacking an N-terminal His tag ( $T_1/T_2 = 4.4$ ,  $\tau_c = 7.0$  ns; data not shown) is consistent with a monomeric protein.

To further investigate the oligomerization state of the UHM, we used sedimentation velocity analytical ultracentrifugation (AUC). The AUC data also indicate a largely monomeric state of the UHM domain (Fig. 1D, solid gray line), whereas partial dimerization is observed at higher protein concentrations (Fig. 1D, dotted gray line). By fitting the AUC data to a monomerdimer equilibrium model, the dimerization constant is estimated to be  $K_{\text{dimer}} = 3-4 \text{ mM}$ . The two central RRM domains of Puf60 were reported to dimerize in the presence of DNA (48). We therefore tested whether a construct comprising RRM1RRM2 and the C-terminal UHM had a tendency to dimerize without DNA or SDS. Our AUC data indicate that this construct is largely monomeric as well (Fig. 1D, solid black line). Taken together, these data demonstrate that Puf60-UHM (in the absence of SDS) and Puf60 RRM1-RRM2-UHM (in the absence of DNA or SDS) are monomeric in solution. Therefore, the UHM dimerization observed in denaturing and reducing SDS-PAGE (21) is presumably induced by the experimental conditions.

The Three-dimensional Structure of the PUF60-UHM—Next, we determined the crystal structure of Puf60-UHM at 2.2 Å resolution. Diffracting crystals could only be obtained using a fusion protein, in which E. coli thioredoxin A (Trx) is connected to the N terminus of Puf60-UHM via a short linker sequence (49). We confirmed that the Trx-UHM construct dimerizes in SDS-PAGE similarly to what is seen for the UHM alone (data not shown).

The asymmetric unit consists of eight Trx-Puf60 fusion proteins arranged in a doughnut shape. Eight Trx molecules are stacked in two layers in the center of the doughnut, surrounded by a ring of eight PUF60-UHM domains (Fig. 2A). Consistent with the NMR secondary chemical shifts, Puf60-UHM adopts a  $\beta$ 1- $\alpha$ A- $\beta$ 2- $\beta$ 3- $\alpha$ B- $\beta$ 4- $\alpha$ C secondary structure. A central fourstranded  $\beta$ -sheet is sandwiched by helices  $\alpha A$  and  $\alpha B$  on one side and helix  $\alpha C$  on the other side (Fig. 2*B*). As seen in other UHM structures (14, 23), Puf60-UHM has an additional strand  $\beta$ 3' adjacent to  $\beta$ 4, which forms a  $\beta$ -hairpin extension to the central four-stranded  $\beta$ -sheet. The  $\beta3'$  strand comprises the conserved Arg-Xaa-Phe motif (RWF 535-537 in Puf60), which plays a crucial role in ULM binding in all known UHM·ULM complexes (14, 15, 23). A unique structural feature of Puf60-UHM is the presence of unusually long  $\beta$ 2 and  $\beta$ 3 strands, which form a  $\beta$ -hairpin that protrudes out of the  $\beta$ -sheet (Fig. 2*B*). In solution, the acidic  $\beta$ 2- $\beta$ 3 loop is flexible, as indicated by low heteronuclear NOE values, which drop to a minimum of 0.12 for Gly<sup>504</sup> (Fig. 1B). In contrast, an average heteronuclear NOE of 0.74 for residues 462–501 and 512–559 indicates the absence of internal motion on subnanosecond time scales.

Dimerization Interface—Because Puf60-UHM crystallizes at concentrations above the dimerization constant of 3-4 mm (1.5 mm in the mother liquor, 32 mm in the crystal lattice), we expected to detect a dimeric UHM in the crystal. Analysis with PISA (50) shows that each of the eight Puf60-UHM domains contacts three other Puf60-UHM domains, two in the same and one in a symmetry-related asymmetric unit. One of the UHM-UHM interfaces within an asymmetric unit is composed of charged interactions between the residues EEE (505-507) in the  $\beta$ 2- $\beta$ 3 loop of one protein monomer and Arg<sup>467</sup>, Arg<sup>540</sup>/ Lys $^{541}$  in the adjacent strands  $\beta1$  and  $\beta4$  of the other dimer subunit, respectively (Fig. 2C). As shown in the electrostatic surface representation (Fig. 2C, right panel), the residues Arg467, Arg540, and Lys541 form a positively charged surface, which is contacted by the negatively charged acidic  $\beta$ 2- $\beta$ 3 loop. The electrostatic interactions involve the tips of the long side chains of arginine/lysine, which contact glutamate/aspartate residues in the mobile  $\beta$ 2- $\beta$ 3 loop. Of the six salt bridges that can be formed, electron density is visible for a maximum of four contacts in any of the putative dimer interfaces in the asymmet-



<sup>&</sup>lt;sup>b</sup> As defined in REFMAC (41).

<sup>&</sup>lt;sup>c</sup> Residual isotropic B-factor after TLS refinement.

<sup>&</sup>lt;sup>d</sup> As defined in PROCHECK (59).

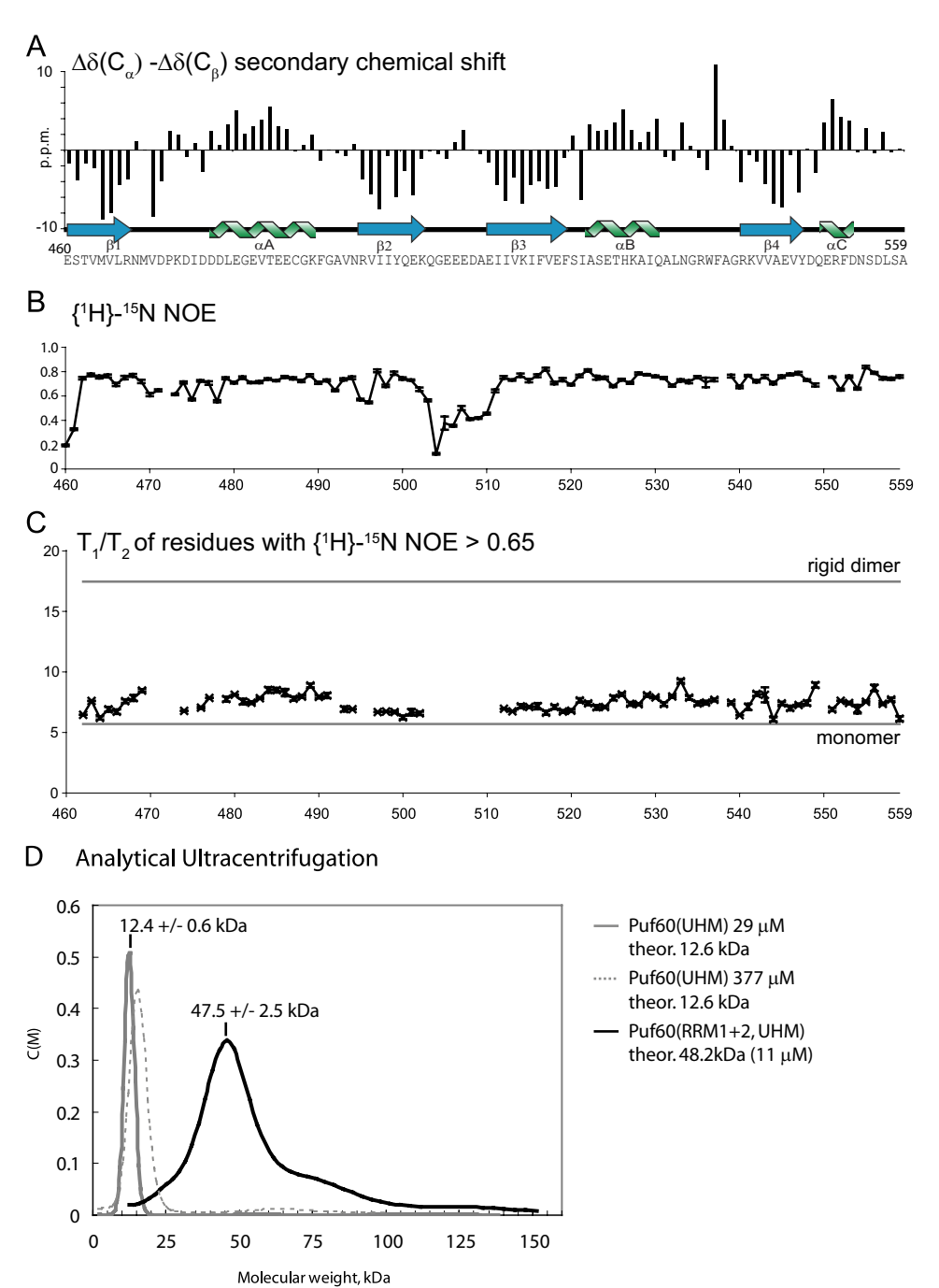


FIGURE 1. **NMR analysis of Puf60-UHM.** All of the experiments were recorded at 297, on a Bruker DRX500 spectrometer using standard experiments (33). *A*, secondary chemical shifts  $\Delta\delta(^{13}C\alpha^{-13}C\beta)$  reveal secondary structure as indicated below the graph with the primary sequence of Puf60-UHM. *B*,  $^{1}$ H- $^{15}$ N heteronuclear NOE of Puf60-UHM. C, ratio of  $^{15}$ N  $T_1$  and  $T_2$  relaxation times for residues with  $^{1}$ H- $^{15}$ N >0.65. The gray horizontal lines depict expected average values for a 12.6-kDa monomer and a 25-kDa dimer at 297 K and 50.68 MHz Larmor frequency, calculated as in Refs. 44 and 45. D, analytical ultracentrifugation analysis of Puf60-UHM (solid gray line, concentration 29  $\mu$ M; dotted gray, 377  $\mu$ M) and a construct comprising the two central RRM domains and the UHM of Puf60 (black line, 11 μM). The expected theoretical molecular masses are given on the right.

ric unit. Notably, the combinations of charged residues involved in direct salt bridges vary for the different dimer interfaces in the asymmetric unit.

To determine which residues are involved in the dimerization of Puf60 in SDS-PAGE, we introduced amino acid changes for the residues in the  $\beta$ 2- $\beta$ 3 loop (E501A/K502A/Q503A, E505A/E506A/E507A, and D508A/A509A/E510A) and of the positively charged residues that contact the acidic loop (R540A/

K541A, R467A, and RK540-541AA+R467A). The structural integrity of the E505A/E506A/ E507A mutant was confirmed by comparison of the HSQC spectra (supplemental Fig. S1). The integrity of the other mutants was confirmed by one-dimensional NMR (data not shown).

In denaturing SDS-PAGE, Puf60-UHM wild type (12.6 kDa), E501A/ K502A/Q503A, R540A/K541A, and R467A run at an apparent molecular mass of 28 kDa (Fig. 2D, lanes 1, 2, 5, and 6, respectively), as expected for a dimer. In contrast, the mutants E505A/E506A/E507A (lane D508A/A509A/E510A (lane 4), and R540A/K541A+R467A (*lane 7*) run at lower molecular masses, indicating that their dimerization is impaired.

These findings indicate that the dimerization of Puf60 UHM involves the acidic residues  $^{505}$ EEEDAE $^{510}$  in the flexible  $\beta$ 2- $\beta$ 3 loop and the basic residues Arg467 and Arg<sup>540</sup>-Lys<sup>541</sup>. Salt bridges and electrostatic contacts between these regions thus mediate dimerization of Puf60-UHM in the presence of SDS and presumably also contribute to the small population of dimeric species in physiological buffers (Fig. 1D).

To confirm that the observed bands indeed correspond to dimerization of the UHM in SDS-PAGE and that the observed positions of the bands do not fortuitously appear at unusual positions, we mixed recombinant, purified ZZ-tagged wild type UHM (28.4/56.8 kDa for monomer/dimer; Fig. 2E, lane 1) with untagged wild type UHM (12.6/25.2 kDa; Fig. 2E, lane 6). Because the protein species at 41.2 kDa in lanes 2 and 3 is not contained in either pure ZZ-tagged UHM (lane 1) or untagged UHM (lane 6),

the appearance of a mixed dimer species of the type ZZ-UHM·UHM at 41.2 kDa (lanes 2 and 3) proves the formation of a mixed dimer. The UHM mutant E505A/E506A/E507A does not form the mixed dimer species, confirming that the mutations impair the dimerization of the UHM in SDS-PAGE (Fig. 2E, lanes 4, 5, and 7).

SDS Induces the Dimerization of Wild Type Puf60 UHM—To gain some insight into the molecular basis of the SDS-induced

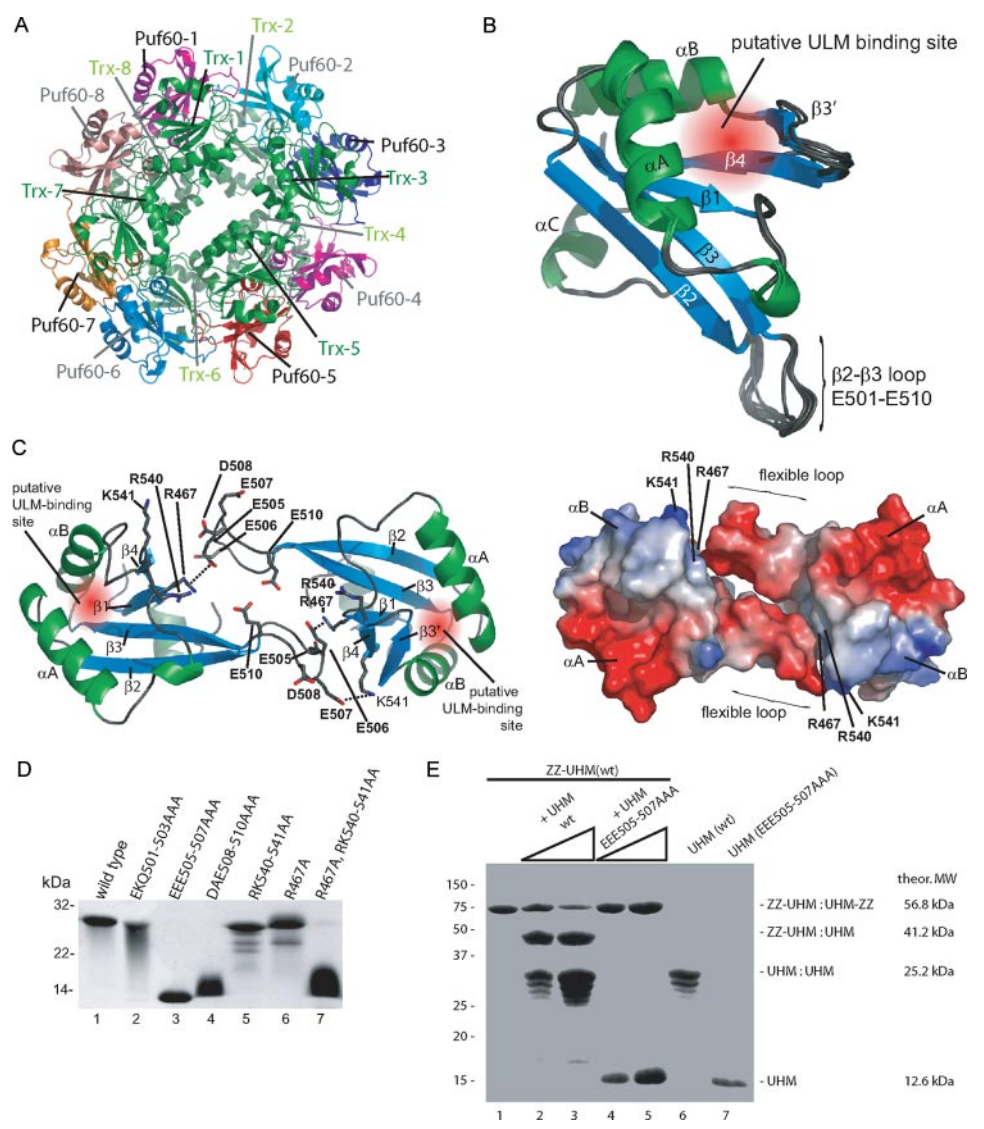


FIGURE 2. Crystal structure of Puf60-UHM. A, the asymmetric unit consists of eight Trx-Puf60 fusion proteins arranged in a doughnut shape. The Trx domains are shown in green, and the Puf60-UHM domains are shown in different colors. Trx and Puf60 domains with the same number constitute the same peptide chain. B, eight Puf60-UHM domains in the asymmetric unit of the crystal structure are superimposed and shown in a cartoon representation. The putative ULM-binding site (based on known UHM-ULM complex structures) is highlighted by a red sphere. C, putative Puf60-UHM homodimer. Left panel, cartoon representation. The side chains of residues discussed in the text are shown and labeled, and salt bridges are indicated by dashed lines. Right panel, surface electrostatics representation of the dimer shown on the left, in the same orientation. D, mutational analysis of the dimerization interface. Denaturing, Coomassie-stained SDS-PAGE of bacterially expressed and purified Puf60-UHM mutants as denoted on top of the lanes. E, dimerization of Puf60-UHM in SDS-PAGE. Purified, ZZ-tagged UHM was analyzed on Coomassie-stained SDS-PAGE in the absence and presence of increasing amounts of untagged UHM (wild type (wt) and E505A/E506A/E507A mutant), as indicated above the lanes. theor.MW, theoretical molecular mass.

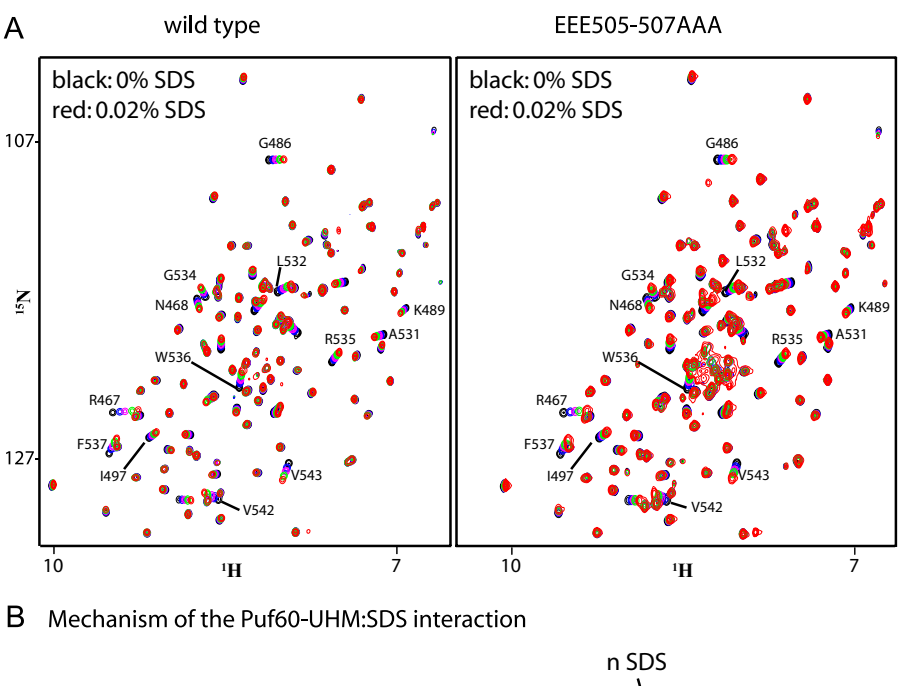
dimerization of Puf60, we monitored the NMR signals of <sup>15</sup>Nlabeled, wild type and mutant (E505A/E506A/E507A) Puf60-UHM in a series of <sup>1</sup>H-<sup>15</sup>N correlation spectra upon titration of increasing amounts of SDS (Fig. 3 and supplemental Figs. S2 and S3). Wild type and mutant UHM bind SDS in a 1:1 ratio and with a  $K_d$  of 24  $\pm$  4 and 45  $\pm$  6  $\mu$ M, respectively (supplemental Fig. S2A). Surprisingly, the binding site overlaps with the putative ULM-binding site of Puf60-UHM (supplemental Fig. S2B). The  $^{15}$ N  $T_1/T_2$  ratio of SDS-bound Puf60-UHM (0.07% (w/v) SDS/2.4 mm/8-fold molar excess) indicates a monomeric protein ( $T_1/T_2 = 4.6$ ,  $\tau_c = 7.2$  ns; supplemental Fig. S2*C*). Thus, a simple equimolar binding of SDS does not induce dimerization

of Puf60-UHM. However, intermediate SDS concentrations (>0.02% (w/v) SDS,  $\sim$ 3-fold molar excess) induce dimerization of the wild type protein, as indicated by the appearance of new signals in the NMR spectra that have 15N NMR relaxation properties expected for a dimer (supplemental Fig. S3). With further increasing SDS concentrations, both Puf60-UHM wild type as well as the mutant protein are denatured (Fig. 3B).

Binding of Puf60 UHM to Tandem ULMs—The dimerization propensity of Puf60-UHM opens the possibility that simultaneous binding of two UHM domains to two adjacent ULMs on the same peptide chain (tandem ULM motif) could cooperatively induce the dimerization also in the absence of SDS. Based on the distance of the ULMbinding sites of the Puf60 homodimer in the crystal structure, we estimated that the ULMs should be separated by a minimum of 15-20 residues in an extended conformation. We identified evolutionarily conserved tandem ULMs in intrinsically disordered regions of several proteins with the program SIRW (51). Of these, tandem ULMs in SF3b155 (194-229, 210-251 and 229-269) and in the nuclear RNA helicase Prp16 (201–238) (Fig. 4, A and B) were tested experimentally for binding to Puf60-UHM.

Using Western blot detected GST pulldown experiments, we found that the tandem ULM sequence of SF3b155 (194-229) binds Puf60-UHM (supplemental Fig. S4A). However, ITC (supplemental Fig. S4, C and D) and NMR (supplemental Fig. S5A) data show that the

binding of Puf60-UHM to SF3b155 (194-229) is mediated by the ULM around Trp<sup>200</sup> and that the ULM at Trp<sup>218</sup> does not contribute to the binding cooperatively. NMR titrations reveal a weak interaction of Puf60-UHM with Prp16 (201-238), which was not detected in the GST pulldown experiments. However, the two ULMs (Trp<sup>215</sup> and Trp<sup>230</sup>) in Prp16 do not mutually enhance each other's binding cooperatively (supplemental Fig. S5B). Thus, dimerization of Puf60-UHM is not induced upon binding to these tandem ULMs in the absence of SDS. ULM binding in the presence of SDS (350 µM to 1.4 mm) was not observed in GST pulldown experiments (data not shown). This is consistent with the observation that the SDS interaction



UHM + SDS ← UHM\*SDS ← unfolded UHM wild type: (UHM\*SDS)<sub>3</sub>\*SDS<sub>2</sub> **EEE** UHM + SDS ← UHM\*SDS ← unfolded UHM 505-507: AAA

FIGURE 3. SDS binding of Puf60-UHM. A, overlays of HSQC spectra of 15N-labeled Puf60-UHM wild type (left) and triple mutant E505A/E506A/E507A (right) at SDS concentrations between 0% (black) and 0.02% (3-fold molar excess, red). B, proposed model  $\overline{f}$ or the interaction between Puf60-UHM and SDS. In both wild type and mutant UHM, a single SDS molecule can bind to the hydrophobic ULM-binding pocket (supplemental Fig. 2B). SDS-bound wild type Puf60-UHM, but not E505A/E506A/E507A, can dimerize at intermediate SDS concentrations. High SDS concentrations lead to unfolding of wild type and mutant UHM domain (supplemental Fig. 3).

maps to the canonical ULM-binding site of Puf60-UHM (supplemental Fig. S2B) and thus that SDS and ULM binding are competitive.

Distinct ULM Binding Properties of Puf60 and U2AF<sup>65</sup>—GST pulldown experiments show that Puf60-UHM binds to ULMs in SF1, U2AF<sup>65</sup>, and SF3b155 (supplemental Fig. S4A). We quantified the affinities of Puf60-UHM for these ULMs by ITC (Fig. 4C, supplemental Fig. 4C, and Table 2). Whereas Puf60-UHM binds to SF1 with a dissociation constant  $K_d = 20.8 \pm 5.2$  $\mu$ M, its binding to U2AF<sup>65</sup>-ULM is almost 8-fold stronger ( $K_d$  =  $2.7 \pm 0.2 \mu M$ ). The binding to the ULM comprising Trp<sup>200</sup> in SF3b155(194-229) is  $\sim$ 5-fold stronger than to the ULM around Trp<sup>338</sup> in SF3b155(317–357) ( $K_d = 1.2 \pm 0.1$  and 5.6  $\pm$  $0.6 \mu M$ , respectively).

The ULM binding preferences of Puf60-UHM are distinct from those of U2AF<sup>65</sup>-UHM (supplemental Fig. S4B and Table 2). As reported previously, U2AF<sup>65</sup>-UHM preferentially binds the ULMs in SF1 (8, 15) and SF3b155(317-357) (13, 18, 24). Of the ULMs in SF3b155, U2AF<sup>65</sup>-UHM binds to the ULM around Trp $^{338}$  ( $K_d=6~\mu{\rm M}$  (18)) with higher affinity than to the one at Trp $^{200}$  ( $K_d=16~\mu{\rm M}$  (18)). This preference is weak

but reproducible (supplemental Fig. S4B) and has been described previously (18).

ULM-binding Site Mapping on Puf60-UHM-We used NMR titrations to map the ULM-binding site onto the structure of Puf60-UHM. Unlabeled peptides comprising the ULMs in SF1(1-25), SF3b155(194-SF3b155(317-357), U2AF<sup>65</sup>(85-112) were titrated to <sup>15</sup>N-labeled Puf60-UHM, chemical shift perturbations were monitored in 1H-15N correlation spectra (Fig. 5A). Mapping the chemical shift perturbations onto the crystal structure of Puf60-UHM shows that for all four ULMs, the strongest chemical shift perturbations cluster around the  $\beta$ 1- $\alpha$ A loop, helix  $\alpha A$  and around the RWF motif (part of helix  $\alpha B$  and strands  $\beta3'$  and  $\beta4$ ) of Puf60-UHM (Fig. 5B). The ULM interaction interface of Puf60-UHM is thus analogous to the interfaces of the U2AF35-UHM·U2AF<sup>65</sup>-ULM (20),U2AF<sup>65</sup>-UHM·SF1-ULM (15), and the SPF45·SF3b155(330-342) (23) complexes, indicating a similar mode of molecular recognition.

Structural Basis for ULM Specificity—To further characterize the binding specificity of Puf60-UHM for distinct ULMs we compared its structure with the structures of the UHM·ULM com-

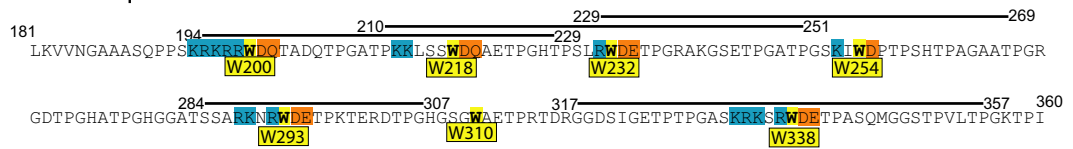
plexes of U2AF<sup>65</sup>·SF1 (Protein Data Bank code 1O0P) and SPF45·SF3b155 (Protein Data Bank code 2PEH). As shown in Fig. 5C, the ULM-binding region of Puf60-UHM, defined by the NMR titrations (Fig. 5B), is structurally more similar to SPF45 than to U2AF $^{65}$ . Helix  $\alpha A$  in U2AF $^{65}$ -UHM is N-terminally extended by four additional residues compared with the  $\alpha$ A helices in Puf60-UHM and SPF45-UHM. As a conseguence, the conformation of the  $\beta$ 1- $\alpha$ A loops in U2AF<sup>65</sup>-UHM differs considerably from Puf60-UHM or SPF45-UHM. It is likely that these differences, in combination with amino acid variations in the ULM sequences (Fig. 4A), determine the specificity of the UHM·ULM complexes. For example, SF1 has a longer stretch of positively charged residues preceding the ULM-tryptophan than the SF3b155 ULMs. In the U2AF<sup>65</sup>·SF1 structure, this region contacts the highly negatively charged helix αA of U2AF<sup>65</sup>-UHM (10 Glu/Asp residues). Because the length helix  $\alpha A$  of Puf60 is shorter and because it is less negatively charged (5 Glu/Asp residues), ionic interactions involving these residues should contribute less to the ULM binding by Puf60-UHM. A second specificity-mediating region in the SF1 and SF3b155 ULMs involves



#### A Putative ULM Sequences



#### B Partial Sequence of the SF3b155 N-terminal Domain



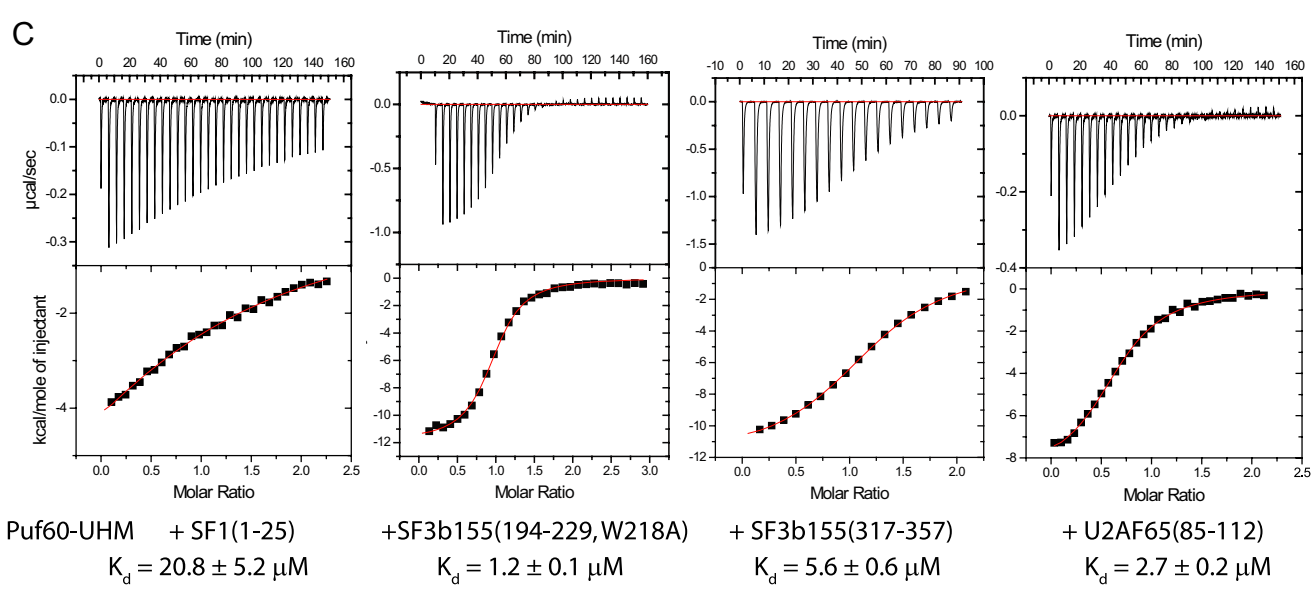


FIGURE 4. **Binding of Puf60-UHM to various ULMs.** A, sequence alignment of ULMs. The conserved tryptophans are aligned and colored in *yellow*, basic residues preceding the tryptophan are highlighted in *blue*, and [N,Q,D,E]-type residues directly succeeding the tryptophan are in *orange*, and potentially phosphorylated Thr-Pro or Ser-Pro repeats are in *purple*. SF1-Ser<sup>20</sup> (inhibits binding to U2AF<sup>65</sup> when phosphorylated (58)) and serines in analogous positions in other ULMs are colored in *green*. B, partial sequence of the N-terminal domain of SF3b155. The peptides used in GST pulldown experiments are highlighted. Same color code as in A. C, isothermal titration calorimetry of Puf60-UHM with ULM peptides of SF1, SF3b155, and U2AF65. The dissociation constants ( $K_d$ ) are indicated. For SF3b155(194–229) the W218A mutant peptide was used, in which a minor binding site is removed (see supplemental Fig. A, C and D).

**TABLE 2**ULM interactions of Puf60-UHM and U2AF<sup>65</sup>-UHM

Shown are the affinities of Puf60 for various ULMs, measured by ITC. +, interaction detected qualitatively, not quantified (see supplemental Fig. S4B, lane 4).

	SF1(1-25)	SF3b155(194-229)	SF3b155(317-357)	U2AF <sup>65</sup> (85-112)
Puf60-UHM	$20.8 \pm 5.2 \ \mu \text{M}$	$1.0\pm0.2~\mu$ M	$5.6 \pm 0.6 \mu$ M	$2.7\pm0.2~\mu\mathrm{M}$
U2AF <sup>65</sup>	$50 \text{ nm}^a$ ; $23 \text{ nm}^b$	$16 \mu \text{M}^{\dot{c}}$	$6.0~\mu\text{M}^c$	+

<sup>&</sup>lt;sup>a</sup> Filter binding (15).

the residue C-terminal of the tryptophan. The aspartate flanking Trp<sup>338</sup> in SF3b155 forms a salt bridge with the arginine in the SPF45-UHM RYF motif (23). Because of its structural similarities to the UHM of Puf60, we speculate that analogous interactions might stabilize the complexes of Puf60-UHM with the SF3b155-ULMs around tryptophans 200 and 338. Because SF1 has an asparagine instead of aspartate at this position, a similar salt bridge cannot be formed,

which may contribute to the weaker interaction of Puf60-UHM with SF1-ULM.

#### DISCUSSION

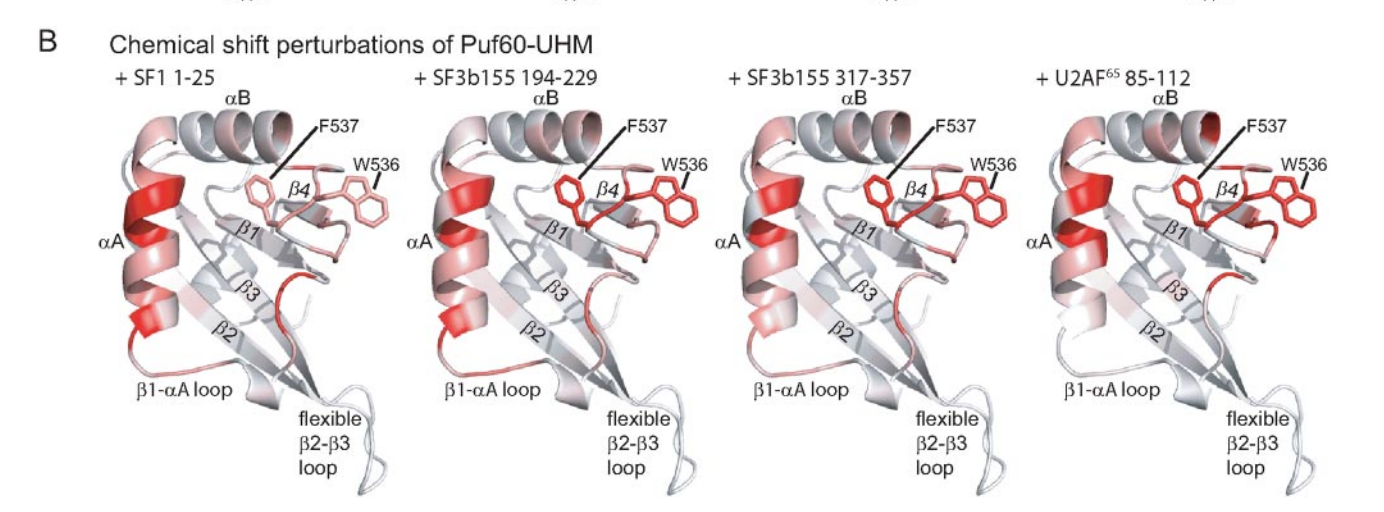
Puf60 was repeatedly found to interact with itself in yeast two-hybrid assays (26, 27), and the Puf60 UHM domain was reported to be necessary and sufficient for the dimerization of Puf60 in SDS-PAGE (21). Our analytical ultracentrifugation



<sup>&</sup>lt;sup>b</sup> ITC (18).

<sup>&</sup>lt;sup>c</sup> Trp fluorescence (18).

# A 1H, 15N HSQC spectra of Puf60-UHM (black) + SF3b155 194-229 (red) +SF3b155 317-357 (red) + U2AF65 85-112 (red)



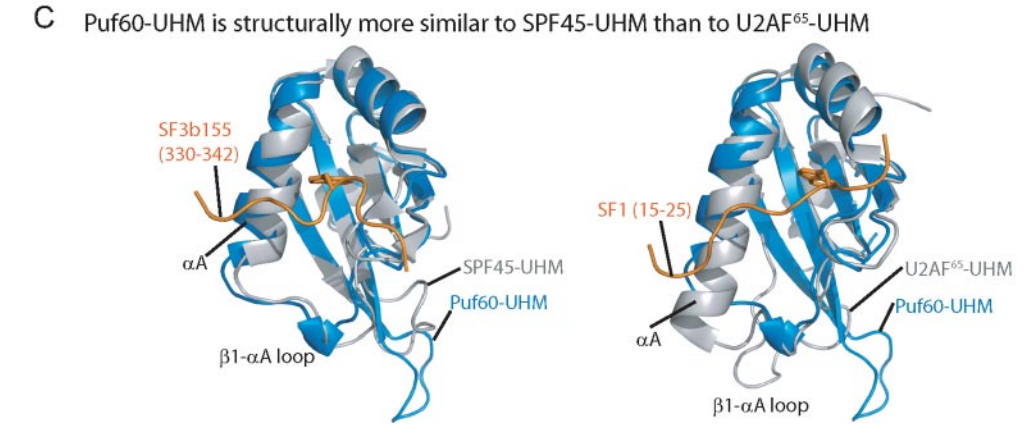


FIGURE 5. NMR chemical shift perturbation of Puf60-UHM/ULM interactions. A, 1H,15N HSQC spectra of free 15N-labeled Puf60-UHM (black) and upon addition of ULM peptides derived from SF1, SF3b155, and U2AF65 (red). B, ribbon representation of the Puf60-UHM structure colored according to the extent of chemical shift perturbation induced by addition of the peptide ligands indicated above (white, no perturbation; red, strong perturbation). C, superposition of the Puf60-UHM structure (blue) onto the structures of SPF45-UHM/SF3b-ULM (left panel, gray; Protein Data Bank code 2PEH) and U2AF65-UHM/SF1-ULM (right panel, gray; Protein Data Bank code 100P).

and NMR data show that the UHM domain is mainly monomeric in physiological buffer, whereas SDS is required for dimerization. A crystal structure and mutational analysis reveal a dimer interface, which is stabilized by electrostatic interactions and involves the acidic  $\beta$ 2- $\beta$ 3 loop of one subunit and basic residues (Lys<sup>467</sup>, Arg<sup>540</sup>, and Lys<sup>541</sup>) in the  $\beta$ -sheet surface of the other subunit of the dimer. The acidic  $\beta$ 2- $\beta$ 3 loop is conserved in all higher eukaryotic orthologs of Puf60 but is distinct in other UHM or RRM domains (20). This suggests that Puf60 orthologs may have a similar dimerization mode, which is unique for Puf60 and not found in other UHMs.

The flexibility of the  $\beta$ 2- $\beta$ 3 loop in solution (indicated by the NMR relaxation data) and the variability of the electrostatic contacts seen in the crystal structure suggest that the dimer interface is dynamic. The electrostatic nature of the dimer interface presumably contributes to the stability of the Puf60-UHM dimer in SDS-PAGE (21) (Fig. 2, D and E). Because the dimerization interface is stabilized by electrostatic contacts, the SDS alkyl chains might not be able to energetically favor the solvation of the UHM monomer.

We found that a longer construct, comprising the two central RRM domains and the UHM, is also largely monomeric in the

H/ppm

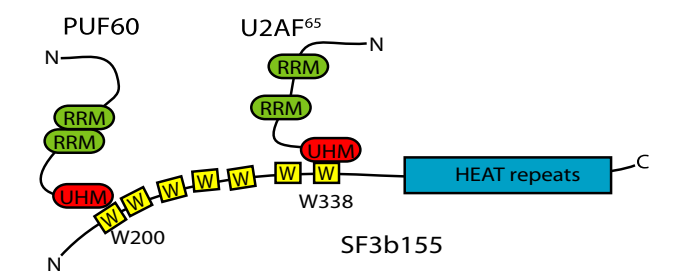


FIGURE 6. Puf60-UHM preferentially binds to the N terminus of SF3b155 at the ULM around Trp<sup>200</sup>, whereas U2AF<sup>65</sup>\_UHM shows preferential binding to the ULM at Trp<sup>338</sup> (18). The domain structure of the proteins is

absence of SDS. Crichlow et al. (48) report a weak tendency of the two central RRM domains to dimerize in the presence of single-stranded DNA. Therefore, it is likely that the oligomerization of Puf60 observed in yeast two-hybrid experiments involves the UHM and the two central RRM domains of Puf60 and additionally requires binding of a ligand. Potentially, ligand-induced dimerization of Puf60-UHM could involve binding of tandem ULMs. However, our experiments with the tandem ULM motifs in SF3b155 and Prp16 did not provide evidence for such a mechanism.

Detergent-induced oligomerization has been reported for several membrane-associated proteins (52–56). No experimental evidence for a functional role of the SDS-induced dimerization of Puf60-UHM is known. However, it is possible that detergent-induced (or lipid-induced) dimerization might play a role for the molecular functions of Puf60. Alternatively, SDS may resemble a putative, as yet unknown ligand of Puf60.

Puf60 was reported to interact directly with U2AF<sup>65</sup> (26, 27). Our data provide a rationale for how the two proteins interact and suggest that a minimal binding interface involves the ULM sequence of U2AF<sup>65</sup> and the UHM domain of Puf60. Note that binding of Puf60 to the U2AF65 ULM can only occur if this ULM is not already bound by U2AF35-UHM, which has a significantly higher affinity. Thus, for this interaction to occur in vivo, there should be a population of U2AF<sup>65</sup> molecules that is not bound to U2AF35 in the nucleus.

It was shown in pulldown experiments from nuclear extract that Puf60 associates with SF3b155 (28). We suggest that this interaction likely involves direct binding of Puf60-UHM to ULM sequences in the N terminus of SF3b155. Interestingly, the Puf60-UHM and U2AF<sup>65</sup>-UHM have distinct binding affinities for ULMs. Puf60-UHM binds only weakly to SF1-ULM, whereas this ULM strongly interacts with U2AF<sup>65</sup>-UHM. Furthermore, Puf60-UHM has a stronger affinity to SF3b155(194-229) than to SF3b155(317–357), whereas the opposite is found for U2AF<sup>65</sup>-UHM (Table 2). The affinity differences of these two UHM domains are rationalized by comparing structural models of these interactions. As shown in Fig. 5C, the ULMbinding region of the two UHMs is significantly different, which may be linked to the distinct binding preferences.

Our biochemical data imply that Puf60 and U2AF<sup>65</sup> can bind to the N terminus of SF3b155 simultaneously and noncompetitively (Fig. 6). The mutual enhancement of splicing activation by these two splicing factors (28) could thus involve simultaneous and potentially cooperative recruitment of SF3b155 to the 3' splice site.

Recently, it was reported that the UHM domain of the kinase KIS strongly binds to SF1 (similar to U2AF<sup>65</sup>-UHM) (22). It also binds to ULMs in the N terminus of SF3b155 and prefers Trp<sup>200</sup> over Trp<sup>338</sup> (similar to Puf60-UHM) (57). The distinct binding preferences of the Puf60, KIS, and U2AF<sup>65</sup> UHMs suggest that UHM-ULM interactions have evolved to achieve some binding selectivity. Thus, a given ULM cannot be classified as strong or weak but might bind with differential affinity to each UHM. Our data provide molecular insights into the intricate network of UHM-ULM interactions. Structure-based analysis allows the design of mutations in ULM and/or UHM sequences for modulating this network and studying its role in the regulation of splicing in vivo.

Acknowledgments—We thank the staff at beam line PX01 of the Swiss Light Source (Villigen, Switzerland) for technical assistance during data collection; Christoph Müller and Stephen Cusack for sharing beam-time; and Juan Valcárcel and Rebecca Wade for discussions and critical reading of the manuscript.

#### REFERENCES

- 1. Brow, D. A. (2002) Annu. Rev. Genet. 36, 333-360
- 2. Berglund, J. A., Chua, K., Abovich, N., Reed, R., and Rosbash, M. (1997) Cell 89, 781-787
- 3. Liu, Z., Luyten, I., Bottomley, M. J., Messias, A. C., Houngninou-Molango, S., Sprangers, R., Zanier, K., Kramer, A., and Sattler, M. (2001) Sciences (N. Y.) **294,** 1098 –1102
- 4. Singh, R., Valcarcel, J., and Green, M. R. (1995) Sciences (N. Y.) 268, 1173-1176
- 5. Wu, S., Romfo, C. M., Nilsen, T. W., and Green, M. R. (1999) Nature 402, 832 - 835
- 6. Merendino, L., Guth, S., Bilbao, D., Martinez, C., and Valcarcel, J. (1999) Nature 402, 838 - 841
- 7. Zorio, D. A., and Blumenthal, T. (1999) Nature 402, 835-838
- 8. Berglund, J. A., Abovich, N., and Rosbash, M. (1998) Genes Dev. 12,
- 9. Query, C. C., Moore, M. J., and Sharp, P. A. (1994) Genes Dev. 8, 587-597
- 10. Query, C. C., McCaw, P. S., and Sharp, P. A. (1997) Mol. Cell. Biol. 17, 2944 - 2953
- 11. Will, C. L., Schneider, C., MacMillan, A. M., Katopodis, N. F., Neubauer, G., Wilm, M., Luhrmann, R., and Query, C. C. (2001) EMBO J. 20, 4536 - 4546
- 12. Schellenberg, M. J., Edwards, R. A., Ritchie, D. B., Kent, O. A., Golas, M. M., Stark, H., Luhrmann, R., Glover, J. N., and MacMillan, A. M. (2006) Proc. Natl. Acad. Sci. U. S. A. 103, 1266-1271
- 13. Gozani, O., Potashkin, J., and Reed, R. (1998) Mol. Cell. Biol. 18, 4752 - 4760
- 14. Kielkopf, C. L., Rodionova, N. A., Green, M. R., and Burley, S. K. (2001) *Cell* **106,** 595–605
- 15. Selenko, P., Gregorovic, G., Sprangers, R., Stier, G., Rhani, Z., Krämer, A., and Sattler, M. (2003) Mol. Cell 11, 965-976
- 16. Rain, J. C., Rafi, Z., Rhani, Z., Legrain, P., and Krämer, A. (1998) RNA (N. Y.) 4, 551-565
- 17. Rudner, D. Z., Kanaar, R., Breger, K. S., and Rio, D. C. (1998) Mol. Cell. Biol. 18, 1765-1773
- 18. Thickman, K. R., Swenson, M. C., Kabogo, J. M., Gryczynski, Z., and Kielkopf, C. L. (2006) J. Mol. Biol. 356, 664 – 683
- 19. Cass, D. M., and Berglund, J. A. (2006) Biochemistry 45, 10092-10101
- 20. Kielkopf, C. L., Lucke, S., and Green, M. R. (2004) Genes Dev. 18,
- 21. Page-McCaw, P. S., Amonlirdviman, K., and Sharp, P. A. (1999) RNA



- (*N. Y.*) **5,** 1548 1560
- 22. Manceau, V., Swenson, M., Le Caer, J. P., Sobel, A., Kielkopf, C. L., and Maucuer, A. (2006) FEBS J. 273, 577-587
- 23. Corsini, L., Bonnal, S., Basquin, J., Hothorn, M., Scheffzek, K., Valcarcel, J., and Sattler, M. (2007) Nat. Struct. Mol. Biol. 14, 620 - 629
- 24. Spadaccini, R., Reidt, U., Dybkov, O., Will, C., Frank, R., Stier, G., Corsini, L., Wahl, M. C., Luhrmann, R., and Sattler, M. (2006) RNA (N. Y.) 12, 410 - 425
- 25. Zhang, M., Zamore, P. D., Carmo-Fonseca, M., Lamond, A. I., and Green, M. R. (1992) Proc. Natl. Acad. Sci. U. S. A. 89, 8769 – 8773
- 26. Poleev, A., Hartmann, A., and Stamm, S. (2000) Eur. J. Biochem. 267, 4002 - 4010
- 27. Rual, J. F., Venkatesan, K., Hao, T., Hirozane-Kishikawa, T., Dricot, A., Li, N., Berriz, G. F., Gibbons, F. D., Dreze, M., Ayivi-Guedehoussou, N., Klitgord, N., Simon, C., Boxem, M., Milstein, S., Rosenberg, J., Goldberg, D. S., Zhang, L. V., Wong, S. L., Franklin, G., Li, S., Albala, J. S., Lim, J., Fraughton, C., Llamosas, E., Cevik, S., Bex, C., Lamesch, P., Sikorski, R. S., Vandenhaute, J., Zoghbi, H. Y., Smolyar, A., Bosak, S., Sequerra, R., Doucette-Stamm, L., Cusick, M. E., Hill, D. E., Roth, F. P., and Vidal, M. (2005) Nature 437, 1173-1178
- Hastings, M. L., Allemand, E., Duelli, D. M., Myers, M. P., and Krainer, A. R. (2007) PLoS ONE 2, e538
- 29. Liu, J., He, L., Collins, I., Ge, H., Libutti, D., Li, J., Egly, J. M., and Levens, D. (2000) Mol. Cell 5, 331-341
- 30. Quinn, L. M., Dickins, R. A., Coombe, M., Hime, G. R., Bowtell, D. D., and Richardson, H. (2004) Development (Camb.) 131, 1411-1423
- 31. Van Buskirk, C., and Schupbach, T. (2002) Dev. Cell 2, 343-353
- 32. Delaglio, F., Grzesiek, S., Vuister, G. W., Zhu, G., Pfeifer, J., and Bax, A. (1995) J. Biomol. NMR 6, 277-293
- 33. Johnson, B. A., and Blevins, R. A. (1994) J. Biomol. NMR 4, 603-614
- 34. Sattler, M., Schleucher, J., and Griesinger, C. (1999) Prog. NMR Spectrosc. **34.** 93–158
- 35. Farrow, N. A., Muhandiram, R., Singer, A. U., Pascal, S. M., Kay, C. M., Gish, G., Shoelson, S. E., Pawson, T., Forman-Kay, J. D., and Kay, L. E. (1994) Biochemistry 33, 5984-6003
- 36. Amezcua, C. A., Harper, S. M., Rutter, J., and Gardner, K. H. (2002) Structure 10, 1349-1361
- 37. Kabsch, W. (1993) J. Appl. Crystallogr. 26, 795-800
- 38. McCoy, A. J., Grosse-Kunstleve, R. W., Adams, P. D., Winn, M. D., Sto-

- roni, L. C., and Read., R. J. (2007) J. Appl. Crystallogr. 40, 658 674
- 39. Sali, A., and Blundell, T. L. (1993) J. Mol. Biol. 234, 779 815
- 40. Emsley, P., and Cowtan, K. (2004) Acta Crystallogr. 60, 2126-2132
- 41. Murshudov, G. N., Vagin, A. A., and Dodson, E. J. (1997) Acta Crystallogr. 53,240-255
- 42. Adams, P. D., Grosse-Kunstleve, R. W., Hung, L. W., Ioerger, T. R., Mc-Coy, A. J., Moriarty, N. W., Read, R. J., Sacchettini, J. C., Sauter, N. K., and Terwilliger, T. C. (2002) Acta Crystallogr. 58, 1948-1954
- 43. Maris, C., Dominguez, C., and Allain, F. H. (2005) FEBS J. 272, 2118 –2131
- 44. Kay, L. E., Torchia, D. A., and Bax, A. (1989) Biochemistry 28, 8972-8979
- 45. Tjandra, N., Wingfield, P., Stahl, S., and Bax, A. (1996) J. Biomol. NMR 8, 273-284
- 46. Fushman, D., Weisemann, R., Thüring, H., and Rüterjans, H. (1994) J. Biomol. NMR 4, 61-78
- 47. Daragan, V., and Mayo, K. H. (1997) Prog. Nuclear Magn. Reson. Spectroscopy 31, 63-105
- 48. Crichlow, G. V., Zhou, H., Hsiao, H. H., Frederick, K. B., Debrosse, M., Yang, Y., Folta-Stogniew, E. J., Chung, H. J., Fan, C., De la Cruz, E. M., Levens, D., Lolis, E., and Braddock, D. (2008) EMBO J. 27, 277-289
- 49. Corsini, L., Hothorn, M., Scheffzek, K., Sattler, M., and Stier, G. (2008) Protein Sci., in press
- 50. Krissinel, E., and Henrick, K. (2007) J. Mol. Biol. 372, 774-797
- 51. Ramu, C. (2003) Nucleic Acids Res. 31, 3771-3774
- 52. Chung, S. H., Weiss, R. S., Frese, K. K., Prasad, B. V., and Javier, R. T. (2008) Oncogene 27, 1412-1420
- 53. Forouhar, F., Huang, W. N., Liu, J. H., Chien, K. Y., Wu, W. G., and Hsiao, C. D. (2003) J. Biol. Chem. 278, 21980-21988
- 54. Bhakdi, S., Fussle, R., and Tranum-Jensen, J. (1981) Proc. Natl. Acad. Sci. *U. S. A.* **78,** 5475–5479
- 55. Forti, S., and Menestrina, G. (1989) Eur. J. Biochem. 181, 767–773
- Ramachandran, R., Tweten, R. K., and Johnson, A. E. (2004) Nat. Struct. Mol. Biol. 11, 697-705
- 57. Manceau, V., Kielkopf, C. L., Sobel, A., and Maucuer, A. (2008) J. Mol. Biol. **381,** 748 – 762
- Wang, X., Bruderer, S., Rafi, Z., Xue, J., Milburn, P. J., Kramer, A., and Robinson, P. J. (1999) EMBO J. 18, 4549 - 4559
- 59. Laskowski, R. A., MacArthur, M. W., Moss, D. S., and Thornton, J. M. (1993) J. Appl. Crystallogr. 26, 283-291



## **Supplemental Data**

## Dimerization and protein binding specificity of the U2AF Homology Motif (UHM) of the splicing factor Puf60

Lorenzo Corsini<sup>1</sup>, Michael Hothorn<sup>1,4</sup>, Gunter Stier<sup>1</sup>, Vladimir Rybin<sup>1</sup>, Klaus Scheffzek<sup>1</sup> Toby J. Gibson<sup>1</sup> and Michael Sattler<sup>1,2,3,5</sup>

Supplementary Fig. 1 - Structural integrity of Puf60-UHM (EEE505-507AAA).

Supplementary Fig. 2 - SDS binding by Puf60-UHM.

Supplementary Fig. 3 - SDS induces the dimerization of wild type Puf60-UHM.

Supplementary Fig. 4 - Binding of the UHMs of Puf60 and U2AF65 to various ULMs.

Supplementary Fig. 5 - Non-cooperative binding of Puf60-UHM to tandem ULMs.

Supplementary Fig. 6 - Binding of the UHM domains of U2AF35 and SPF45 to various ULMs.

#### **Supplementary Methods**

*NMR titrations.* Peptides for NMR titrations were cleaved from the His<sub>6</sub>-GST-tags with TEV protease and the tags were removed with a second Ni-NTA purification step. The peptides were further purified with a cation exchange SP-Sepharose column (HiTrap<sup>TM</sup>), followed by desalting and concentration with reversed-phase disposable columns (Supelco Discovery C18). After elution with 80/19.9/0.1 (v/v/v) acetonitrile/H<sub>2</sub>O/trifluoro acetic acid the solution was dried in a speed-vac before resuspension in PBS buffer.

NMR titrations were performed by adding increasing amounts of ULM peptides from 7-15 mM stock solutions in PBS to  $^{15}$ N-labelled Puf60-UHM (310  $\mu$ M) and monitored using  $^{1}$ H, $^{15}$ N HSQC experiments.

For each titration, if at least 3 peaks were found to shift clearly in the fast exchange regime, a non-linear regression fit against the following equation was used to obtain the corresponding  $K_d$ .  $\Delta \delta = \Delta \delta_{max} \ x \ \{ (L+P+K_d) - [(L+P+K_d)^2 - (4 \ x \ L \ x \ P)]^{0.5} \} / (2 \ x \ P), \qquad where <math display="block">\Delta \delta = sqrt \{ \Delta \delta (^1H)^2 + (0.2*\Delta \delta (^{15}N))^2 \} \text{ is the measured}$ 

chemical shift change at the ligand concentration L and the total protein concentration P, and  $\Delta\delta_{max}$  is the chemical shift change at saturation. Averages and standard deviations of three fitted  $K_d$  values for each ligand are given in the text and in figures.

#### **Supplementary Data**

SDS induces the dimerization of wild type Puf60 UHM. To analyze the SDS-induced dimerization of Puf60 in further detail, we titrated SDS to 15N-labelled, wild type and mutant (EEE505-507AAA) Puf60-UHM and monitored the NMR signals in a series of <sup>1</sup>H, <sup>15</sup>N correlation spectra (Fig. 3A). Surprisingly, wild type and mutant UHM bind SDS in a 1:1 ratio and with a  $K_d$  of 24  $\pm$  4  $\mu M$  and 45  $\pm$  6  $\mu M$ , respectively (Supplementary Fig. 2A). Although EEE505-507AAA binds SDS weaker than wild type, the binding sites coincide, as the same peaks shift in both cases (Fig. 3A). Mapping the chemical shift perturbations onto the structural model of Puf60-UHM shows that helices  $\alpha A$  and  $\alpha B$ , as well as the  $\beta3$ '-strand and the  $\beta3$ '- $\beta4$  loop are mostly affected (Supplementary Fig. 2B, left panel). Comparison with the structure of SPF45-UHM and SF3b155 (330-342) (21) (Supplementary Fig. 2B, right panel) shows that SDS binds into the ULM binding pocket of Puf60-UHM.

The  $^{15}$ N  $^{7}$ T<sub>1</sub> / T<sub>2</sub> ratio of SDS-bound Puf60-UHM (0.07% SDS / 2.4 mM / 8-fold molar excess) shows that it tumbles with a slightly shorter correlation time than Puf60-UHM in the absence of SDS (T<sub>1</sub> / T<sub>2</sub> = 4.6,  $\tau_c$  = 7.2 ns; Supplementary Fig. 2C). Thus, a simple equimolar binding of SDS does not induce dimerization of Puf60-UHM. However, at an SDS-concentration of 850  $\mu$ M (0.02% SDS, 2.9-fold molar excess) a second set of NMR signals emerges (black arrows in Supplementary Fig. 3A, upper panels; see

Supplementary Fig. 3C for the full spectra). The intensity of these peaks is maximal at an SDS-concentration of 2.9 mM (0.1%, 10-fold molar excess) and vanishes at SDS-concentrations above 16 mM (0.5%, 55-fold molar excess). These transiently appearing NMR signals have average  $^{15}$ N relaxation times of  $T_1/T_2$  999 ms/40 ms, corresponding to the relaxation rates expected for a UHM-dimer (218 residues, 297 K, 50.68 MHz:  $T_1/T_2 \sim 859$  ms/48 ms). Thus, the dimerization of PUF60-UHM is induced at SDS concentrations between 850  $\mu$ M and 16 mM.

A third set of signals emerges at an SDS concentration of 0.02% and shows increasing intensity up to an SDS concentration of 1.0% (red arrows in Supplementary Fig. 3B). These signals have average  $T_1/T_2$  of 790 ms/291 ms (data not shown), indicative of fast tumbling typical of an unfolded peptide chain. Apparently, in the presence of SDS, the UHM dimer coexists with the unfolded protein.

In contrast, the mutant EEE505-507AAA, which does not dimerize in SDS-PAGE, unfolds upon addition of SDS, without forming a intermediate dimeric species (Supplementary Fig. 3A, and B, lower panels). Whereas the wild type UHM retains a significant population of folded dimeric species up to an SDS concentration of 3.6 mM (0.10%,12.4-fold molar excess, Supplementary Fig. 3 A and B, upper panels), the mutant is unstructured in SDS concentrations above 2.4 mM (0.07%, 8-fold molar excess). Thus, the mutant is less stable to SDS-denaturation than the wild type protein, indicating that the dimerization of the wild type protein might increase its stability against SDS denaturation.

The melting point of the mutant Puf60-UHM (61°C) is 5°C lower than the melting point of the wild type (data not shown). This indicates that, even though the  $\beta$ 2- $\beta$ 3 loop is highly flexible in solution, it contributes to the stability of Puf60-UHM in the absence of SDS.

Taken together, these data indicate that, at low concentrations, SDS forms a 1:1 complex and binds to the ULM binding site of monomeric Puf60-UHM. Wild type Puf60-UHM, but not the mutant EEE505-507AAA, dimerizes at intermediate SDS concentrations, as shown schematically in Fig. 3B. At higher concentrations, SDS denatures Puf60-UHM wild type as well as the mutant protein.

Binding to tandem ULMs. To test whether the binding of Puf60-UHM to SF3b155 (194-229) is cooperative, we separately mutated the two tryptophans in the tandem ULM peptide (W200 and W218) to alanine and compared the binding affinities of the two mutant peptides to the wild type. If the binding was cooperative, the Gibbs free energies of the single binding events would add and the K<sub>d</sub> of the wild type should be significantly lower than for the two (single) tryptophan mutants. ITC indicates that Puf60-UHM binds wild type SF3b155(194-229) at two sites with highly different affinities (1.0 +/- 0.2  $\mu$ M and 178 +/- 107  $\mu$ M, Supplementary Fig. 4C). The mutant peptide W218A has a single binding site with a  $K_d$  of 1.2 +/- 0.1  $\mu$ M (Supplementary Fig. 4D), which indicates that the ULM around W200, which has more basic residues than the ULM around W218 (Fig. 4A), mediates the binding of the wild type peptide SF3b155(194-229).

NMR titrations indicate that the dissociation constants for the wild type and the W218A mutant are similar within experimental error (0.89 $\pm$ 0.41  $\mu M$  and 0.78 $\pm$ 0.36  $\mu M$ , respectively), whereas the W200A mutant has a  $K_d$  of 83 $\pm$ 40  $\mu M$  (Supplementary Fig. 5A). As the ITC results predicted, this indicates that the ULM at W200 is the main interacting region, and that the second ULM around W218 does not contribute cooperatively to the binding.

The two putative ULMs in Prp16 have low similarity to the ULM consensus when compared to the established ones (Fig. 4A). Consistently, no interaction of Puf60-UHM and Prp16(201-238) found in GST-pulldown experiments (Supplementary Fig. 4A). Prp16(201-238) binds to Puf60-UHM with a  $K_d$  of 207±108  $\mu M$  in NMR titrations (Supplementary Fig. 5B). The Prp16 W215A and W230A mutants have K<sub>d</sub> values of 594±119 µM and 524±382 µM, respectively, indicating that both tryptophans are involved in binding Puf60-UHM (Supplementary Fig. 5B). Taking into account that the wild type sequence contains two ULM sites per peptide, we multiplied the measured peptide concentration by two to estimate an average K<sub>d</sub> per ULM. This yields K<sub>d</sub>  $_{average}$  = 659±112  $\mu M$ . Since the addition of the Gibbs free energies of the two binding sites

interacting with one molecule would roughly correspond to a multiplication of the K<sub>d</sub> values, the data do not support a cooperative binding of the tandem ULMs in Prp16 to a Puf60-UHM dimer.

We conclude that binding of the tandem ULM sequences in SF3b155 or Prp16 is not sufficient to induce the dimerization of Puf60-UHM in solution in the absence of SDS.

*ULM* binding specificity. GST-pulldown experiments show binding of Puf60-UHM to SF1 (1-25, Supplementary Fig. 4A, lane 4), SF3b155(194-229) (lane 5), SF3b155 (317-357, lane 8) and U2AF<sup>65</sup> (85-112, lane 13). A summary of the interactions of Puf60-UHM to various ULMs is given in Supplementary Table 1.

We also compared ULM binding of Puf60-UHM with the interaction of U2AF<sup>65</sup>-UHM to the same ULMs. As reported previously, U2AF<sup>65</sup>-UHM preferentially binds the ULMs in SF1 (Supplementary Fig. 4B, lane 5) (8,15), and SF3b155(317-357) (lane 15) (13,22,55). U2AF<sup>65</sup>-UHM also can mediate an "intramolecular" interaction to the ULM in its own N-terminus (85-112) (lane 4). The preference of U2AF<sup>65</sup>-UHM for the ULM around W338 in the SF3b155 N-terminus over the one at W200 (Supplementary Fig. 4B, compare lanes 11 and 15) is weak but reproducible, and has been described previously (55).

Our GST-pulldown experiments also show binding of both Puf60-UHM and U2AF<sup>65</sup>-UHM to

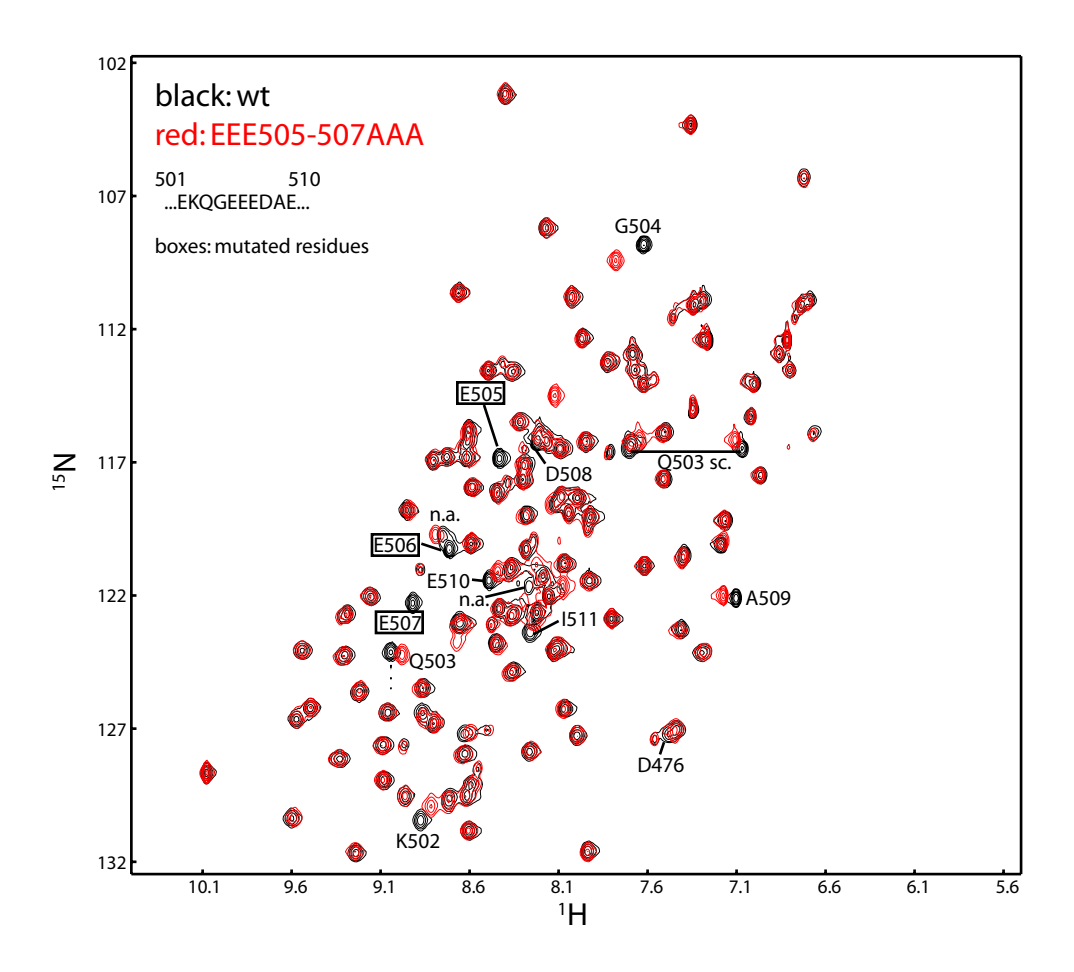
the intrinsically unstructured N-terminus of Prp16 (Supplementary Fig. 4A, lane 10 and 4B, lane 7). However, this binding does not involve the tandem-ULM containing region 201-238 (Supplementary Fig. 4A, lane 9 and 4B lane 6). The sequence of Prp16 comprising residues 1-200 and 239-314 contains four tryptophan residues with weak similarity to ULM sequences, and we suppose that one of these putative ULM sequences mediates binding to the two UHM domains.

To better compare our results with previous literature, we characterized the interactions between the ULMs of SF1, U2AF<sup>65</sup> and SF3b155 and the UHMs of U2AF<sup>35</sup>, and SPF45. As shown in Supplementary Fig. 6, U2AF<sup>35</sup>-UHM binds strongly to U2AF<sup>65</sup>-ULM (compare lanes 3 to 1 and 2), but also reproducibly shows weak binding affinity to SF1 and SF3b155 in GST-pulldowns (lanes 4-6). SPF45-UHM binds to U2AF<sup>65</sup>-ULM (compare lane 10 to 8 and 9), SF1-ULM (lane 13), and the ULM at SF3b155-W338 (lanes 11-12) as described by Corsini et al. (21). Supplementary Table 1 summarizes all of the UHM/ULM interactions that were probed in this article, involving the splicing factors Puf60, U2AF<sup>65</sup>, U2AF<sup>35</sup>, SPF45, SF1, and SF3b155.

#### Supplementary Table 1

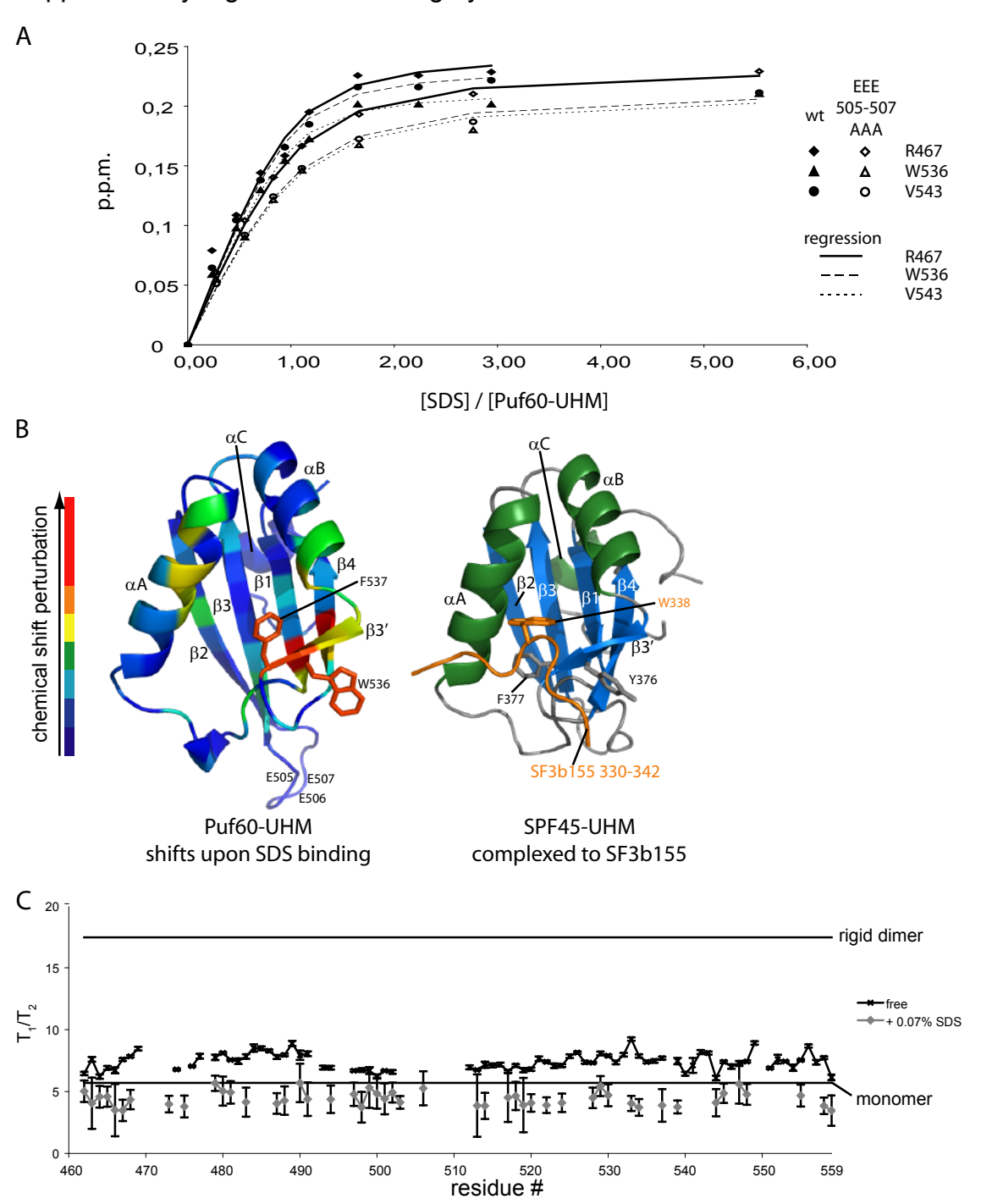
	U2AF <sup>65</sup>	U2AF <sup>35</sup>	SPF45		Puf60-		
	UHM	UHM	UHM		UHM		
	GST-pulldown				NMR-titration	ITC (μM)	
U2AF <sup>65</sup> -ULM (85-112)	++ a	++ <sup>f</sup>	+ f	+ a	binding, i.e. c	2.7±0.2 μM <sup>e</sup>	
SF1-ULM (1-25)	++ a	0/+ f	+ f	+ a	$K_d = 6.5 \pm 1.8 \mu M^c$	20.8±5.2 μM <sup>e</sup>	
SF3b155 (194-229)	- a			+ a	$K_d = 0.9 \pm 0.4  \mu M^{c,d}$	$1.0 \pm 0.2 \mu\text{M}^{\text{e, g}}$	
W218A				+ b	$K_d = 0.8 \pm 0.4  \mu M^d$	$1.2 \pm 0.1  \mu M^{g}$	
W200A				b	$K_d = 83 \pm 40 \mu M^d$	n.d.	
SF3b155 (210-251)	_ a			- a			
comprises W218 and W232							
SF3b155 (229-269)	_ a			- a			
conprises W232 and W254							
SF3b155 (284-307)	_ a						
conprises W293							
SF3b155 (317-357)	- a	0/+ f	+ f	+ a	binding, i.e. c	$5.6 \pm 0.6 \mu M^{e}$	
conprises W338						·	
SF3b155-1-424	+ a						
Prp16 (201-238)	_ a			- a	$K_d = 256 \pm 110 \mu M^d$		
W230A					$K_d = 378 \pm 166 \mu M^d$		
W215A					$K_d = 688 \pm 314 \mu M^d$		
Prp16-1-314	+ a			+ a	·		

Supplementary Table 1: Network of UHM/ULM interactions as detected by GST-pulldown experiments, NMR titrations, and ITC. Legend: ++ strong binding; + binding; 0/+ weak binding; 0 no binding; no entry: not determined.  $K_d$  values were derived by HSQC-titrations if 3 or more peaks shifted in the fast exchange regime. Intermediate exchange (i.e.): strong binding detected by NMR titration, but  $K_d$  values could not be fitted. <sup>a</sup> Supplementary Fig. 4A or B. <sup>b</sup> data not shown. <sup>c</sup> Fig. 5A. <sup>d</sup> Supplementary Fig. 5. <sup>e</sup> Fig. 4C. <sup>f</sup> Supplementary Fig. 6. <sup>g</sup> Supplementary Fig. 4C/D.

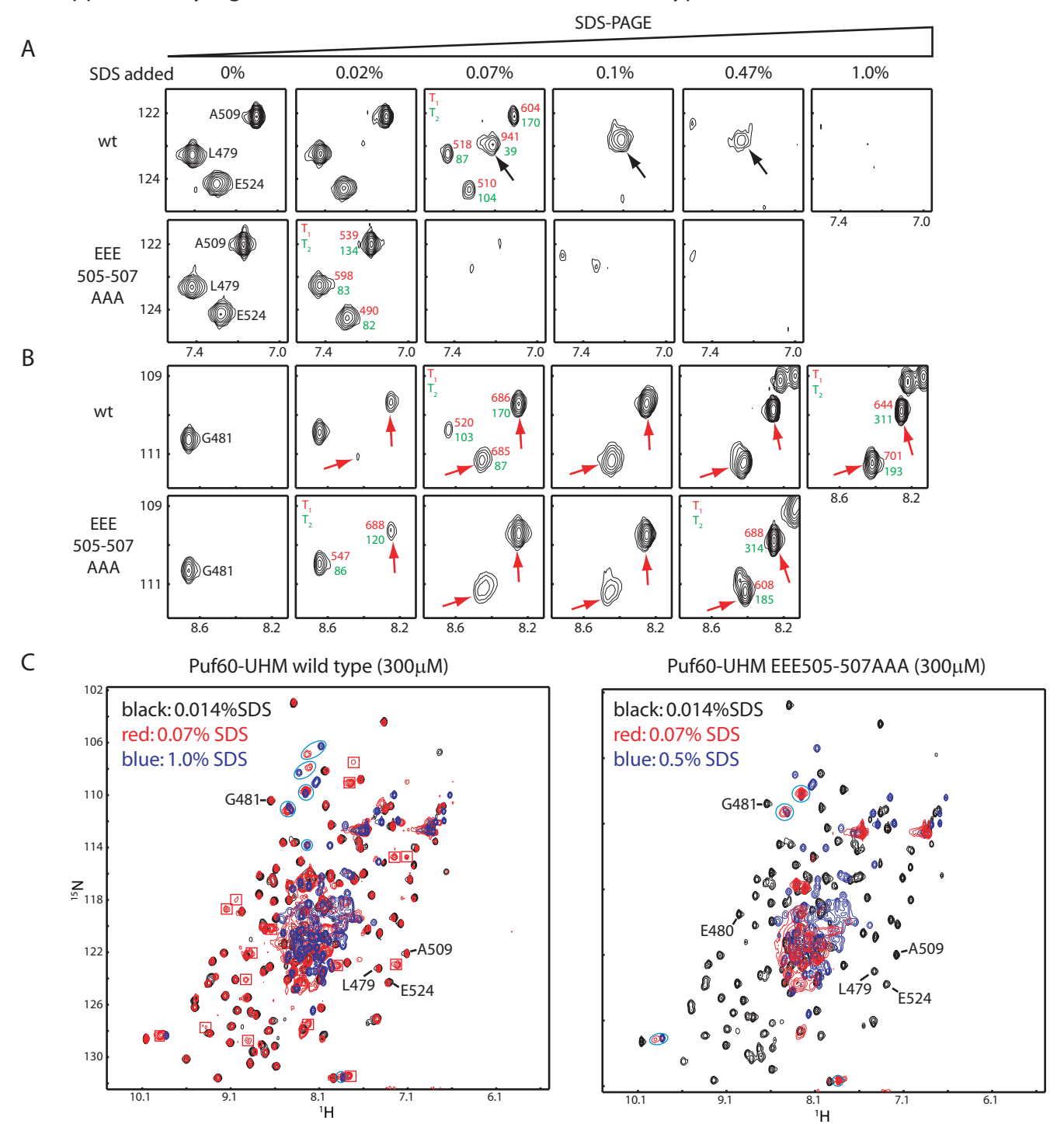


**Supplementary Fig. 1:** Overlay of the HSQC spectra of wild type and EEE505-507AAA Puf60-UHM in the absence of SDS in black and red, respectively. Peaks in the wild type spectrum originating from EEE505-507 are boxed. Peaks originating from residues close to the mutation site are labeled.

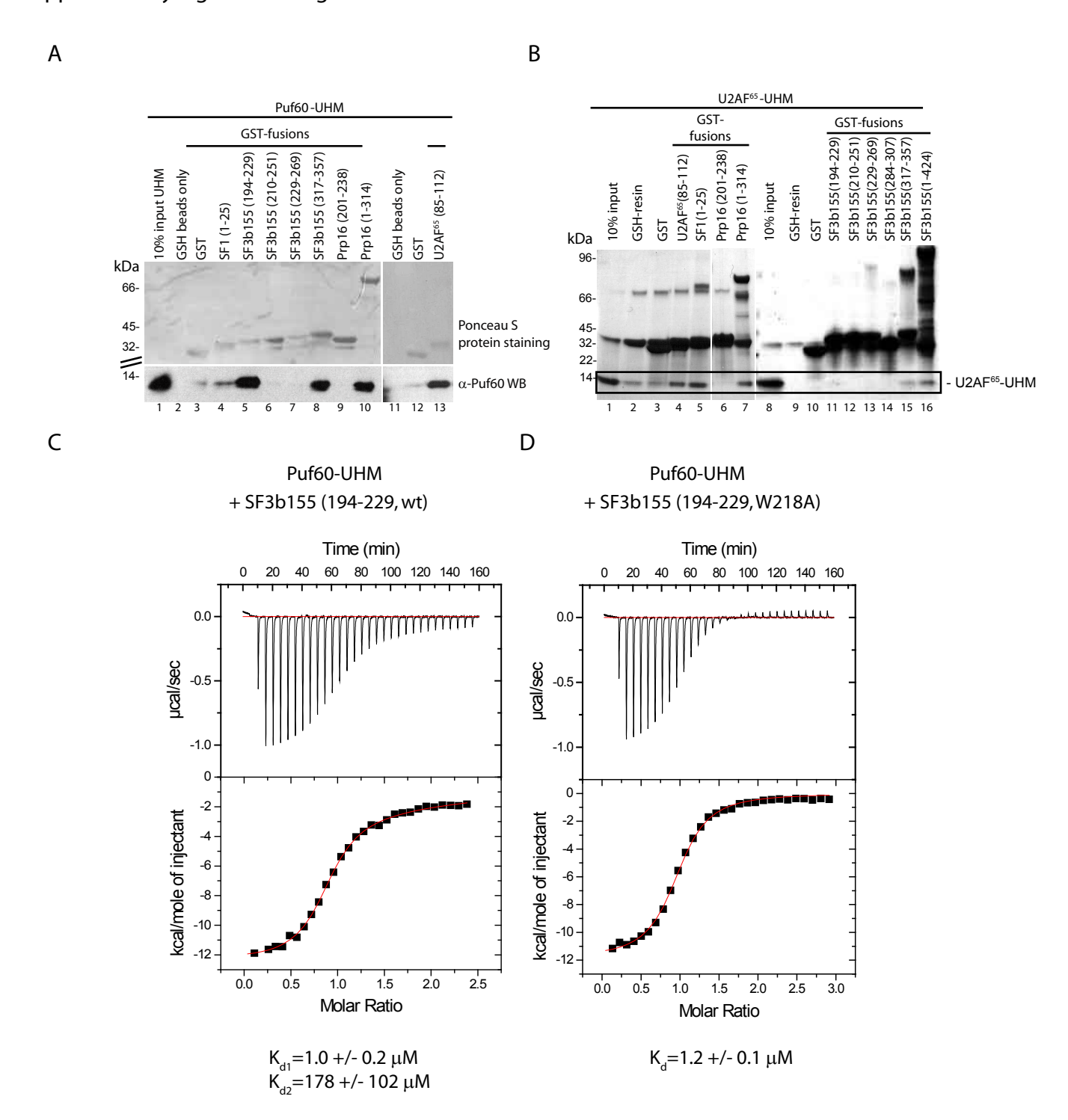
#### Supplementary Fig. 2 - SDS binding by Puf60-UHM



**Supplementary Fig. 2: (A)** Chemical shift perturbation of residues as depicted on the right was plotted over the [SDS]/[Puf60-UHM] concentration ratio (diamonds, triangles and circles). The lines show non-linear regressions to estimate the  $K_{d'}$  as described in Materials and Methods. Wild type and EEE505-507AAA UHM bind SDS in a 1:1 ratio with  $K_{d'}$  values of 24 +/- 4 μM and 45 +/- 6 μM, respectively. **(B)** Chemical shift perturbations upon SDS binding mapped onto the crystal structure of Puf60-UHM cluster in the region where ULM binding is expected. For comparison, the structure of SPF45-UHM (green/blue) bound to a ULM in SF3b155(330-342, orange) is shown on the right. **(C)** <sup>15</sup>N  $T_1/T_2$  ratios of Puf60-UHM free and in presence of 0.07% SDS. The horizontal black lines indicate expected  $T_1/T_2$  ratios for a spherical protein monomer of 109 residues and a 218 residue dimer at 297K and 50.68 MHz Larmor frequency. The  $T_1/T_2$  ratio of SDS-bound Puf60-UHM is lower than what would be expected for a rigid, spherical 109 residue protein, probably because the His<sub>e</sub>-tag and the β2-β3 loop (~17 residues) are flexible.

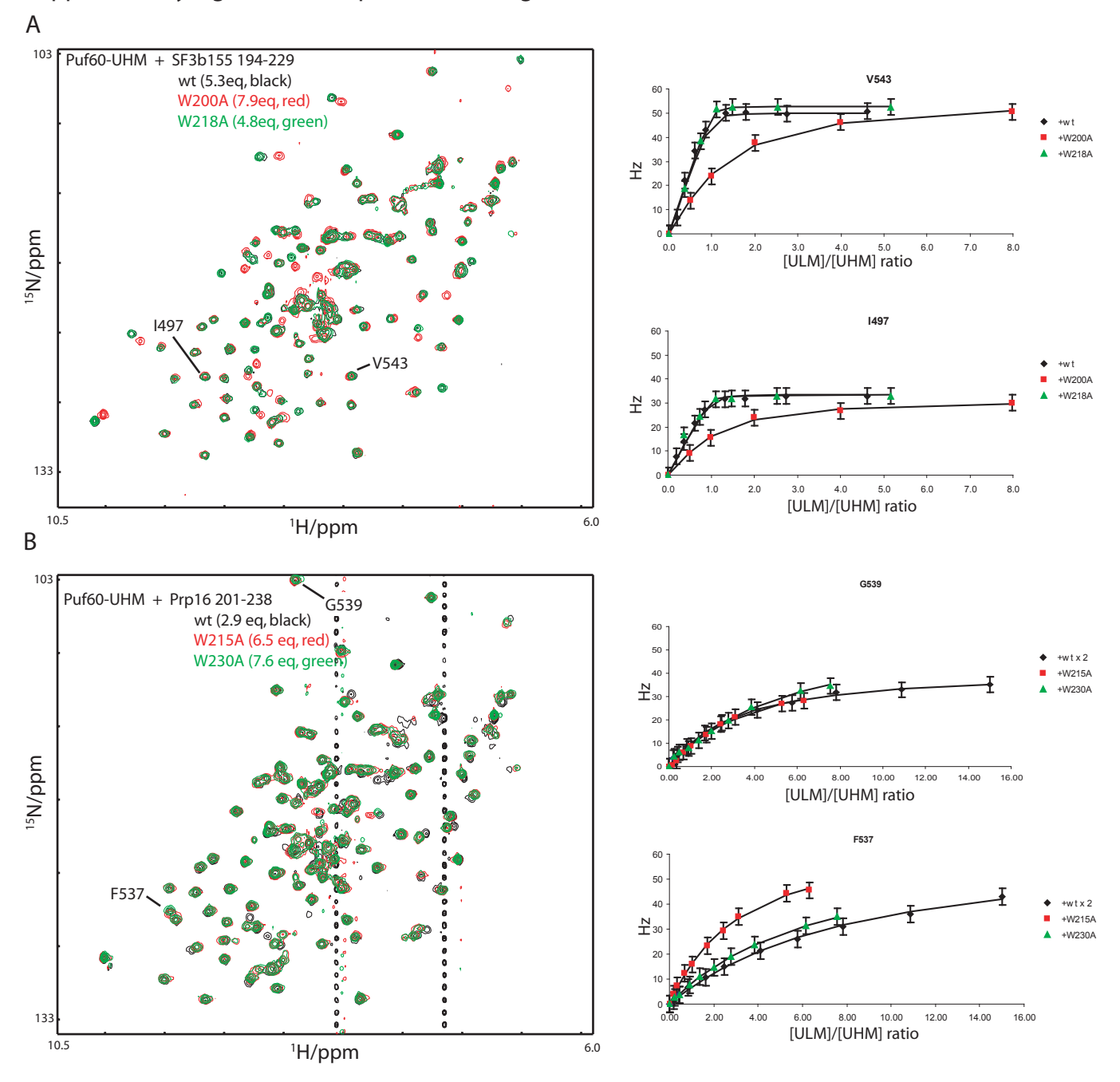


**Supplementary Fig. 3: (A)** Upper panel: Regions of HSQC spectra of wild type Puf60-UHM recorded at the SDS concentrations indicated on top of the graphs. At an SDS concentration of 0.07%, <sup>15</sup>N T1 and T2 were measured, as indicated next to the NMR signals in red and in green, respectively. The black arrows mark signals arising from the SDS-induced Puf60-UHM dimer. Lower panel: a corresponding SDS titration experiment as shown in the upper panel, but with the Puf60-UHM EEE505-507AAA mutant. **(B)** Same in (A), however, in this spectral region, no transiently appearing signals are observed during the SDS titration. The 15N T1 and T2 relaxation times of peaks marked by red arrows are indicative of fast tumbling typical of an unfolded peptide chain. **(C)** Overlay of HSQC spectra of Puf60-UHM wild type or EEE505-507AAA at the SDS concentrations depicted in the legend. Red boxes indicate peaks that appear at 0.02% SDS, have maximal intensity at 0.1% SDS and vanish at concentrations above 0.5%. Blue circles indicate peaks that shift at SDS-concentrations between 0.07% and 1.0%. Peaks arising from residues discussed in the Text and shown in (A) or (B) are labeled.



**Supplementary Fig. 4: (A)** GST-pulldown of Puf60-UHM with several GST-tagged ULMs. Detection of Puf60-UHM was achieved by western blotting, as the much higher concentrations of Puf60-UHM required for coomassie staining induce dimerization of Puf60-UHM in SDS-PAGE. **(B)** GST-pulldown of U2AF<sup>65</sup>-UHM with several GST-tagged ULMs. The band at 32 kDa in lane 1 originates from residual GST, which was not fully separated from U2AF65-UHM during purification. Detection was achieved by coomassie staining, as there is no commercially available antibody for the UHM domain of U2AF<sup>65</sup>. **(C)** ITC of Puf60-UHM and SF3b155 (194-229) wild type. The curve can not be fitted by a single binding-site-model, indicating that both ULM sequences in SF3b155 (194-229) participate in the binding. Fitted dissociation constants for both binding sites are indicated below the graph. **(D)** ITC of Puf60-UHM and SF3b155 (194-229) W218A. In contrast to the curve in (C), this curve is clearly fittable by a single binding-site model. Thus, mutation of the weaker ULM impairs Puf60-UHM binding to the second binding site on the SF3b155 (194-229) peptide, but does not significantly affect binding of the stronger ULM (around W200). This indicates that the binding of Puf60-UHM to SF3b155 (194-229) is non-cooperative.

Supplementary Fig. 5 - Non-cooperative binding of Puf60-UHM to tandem ULMs.

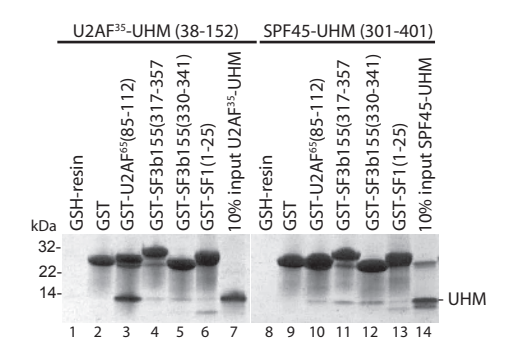


**Supplementary Fig. 5:** HSQC titrations of <sup>15</sup>N labelled Puf60-UHM with unlabelled wt and mutant tandem ULM peptides.

(A) Left: overlay of "titration end-point" HSQC spectra of Puf60-UHM upon addition of saturating amounts of SF3b155 194-229 wild type (black), W200A (red) and W218A (green). On the right, the chemical shift perturbation at various titration points is plottet against the molar ratio of peptide/UHM for V543 (upper graph) and I497(lower graph). The black line depicts the result of the  $\rm K_d$  fitting. Average  $\rm K_d$ s fitted for three peaks in the fast exchange regime for SF3b155(194-229) wild type, W200A and W218A are 0.89+/-0.41 $\mu$ M, 83+/-40 $\mu$ M, and 0.78+/-0.36 $\mu$ M, respectively. Error bars indicate the uncertainties of the measured chemical shifts expressed as the digital resolution of the twice zero-filled spectrum.

(B) Left: overlay of HSQC spectra of Puf60-UHM upon addition of 2.9 molar equivalents of Prp16 201-238 wild type (blue), 6.5 eqivalents of W215A (red) and 7.6 equivalents of W230A (green). On the right, the chemical shift perturbation at various titration points is plottet against the molar ratio of peptide/UHM for G539 (upper graph) and F537(lower graph). The black line depicts the result of the  $K_a$  fitting. The average  $K_a$ s fitted for three peaks in the fast exchange regime for Prp16(301-348) wild type, W215A, and W230A are 207+/-108  $\mu$ M, 594+/-119  $\mu$ M, and 524+/-382  $\mu$ M, respectively. Fitting the  $K_a$  of wild type with the peptide concentration multiplied by two yields an average  $K_a$  per ULM of 659+/-112  $\mu$ M. Error bars indicate the uncertainties of the measured chemical shifts expressed as the digital resolution of the twice zero-filled spectrum.

### Supplementary Fig. 6 - Binding of the UHM domains of U2AF35 and SPF45 to various ULMs



**Supplementary Fig. 6:** Coomassie stained GST-pulldown of U2AF<sup>35</sup>-UHM and SPF45-UHM with various GST-tagged ULM peptides.

## Dimerization and Protein Binding Specificity of the U2AF Homology Motif of the Splicing Factor Puf60

Lorenzo Corsini, Michael Hothorn, Gunter Stier, Vladimir Rybin, Klaus Scheffzek, Toby J. Gibson and Michael Sattler

J. Biol. Chem. 2009, 284:630-639. doi: 10.1074/jbc.M805395200 originally published online October 29, 2008

Access the most updated version of this article at doi: 10.1074/jbc.M805395200

#### Alerts:

- When this article is cited
- · When a correction for this article is posted

Click here to choose from all of JBC's e-mail alerts

#### Supplemental material:

http://www.jbc.org/content/suppl/2008/10/29/M805395200.DC1.html

This article cites 58 references, 14 of which can be accessed free at http://www.jbc.org/content/284/1/630.full.html#ref-list-1